THESIS

FILTRATION EFFICIENCY AND BREATHABILITY OF FABRIC MASKS AND THEIR DEPENDENCE ON FABRIC CHARACTERISTICS

Submitted by

Jacob Fontenot

Department of Mechanical Engineering

In partial fulfillment of the requirements

For the Degree of Master of Science

Colorado State University

Fort Collins, Colorado

Fall 2022

Master's Committee:

Advisor: John Volckens

Ellison Carter
Shantanu Jathar

ABSTRACT

FILTRATION EFFICIENCY AND BREATHABILITY OF FABRIC MASKS AND THEIR DEPENDENCE ON FABRIC CHARACTERISTICS

Throughout the COVID-19 pandemic, the demand for face coverings offering two-way protection significantly increased, which resulted in widespread use of masks made from common fabrics (e.g., wool, cotton, and synthetic materials). However, the effectiveness of these fabric masks, which vary in material and design, is not well understood. This work investigates the performance of fabric masks, namely filtration efficiency and breathability, and their dependence on fabric characteristics. Filtration efficiency (FE) and flow resistance – a measure of mask breathability – were evaluated for 50 fabric masks, followed by individual layer testing (n = 70 total layers). The characteristics of the fabric layers, namely yarn diameter, fiber diameter, thread count, air permeability, porosity, cloth cover factor, infra-red (IR) attenuation, and fabric thickness were quantified in a laboratory setting. Fabric mask FEs were relatively low (i.e., < 50%) for submicron particles but increased with particle diameter. Approximately half of the masks achieved a FE meeting the Level 1 barrier standard specified in ASTM F3502-21. The FE and flow resistance of the component fabric layers was found to accurately predict the FE and flow resistance of the entire mask; therefore, we find that fabric masks can generally be treated as filters in series. FE exhibited the strongest relationship with cloth cover factor, IR attenuation, air permeability, and the number of fabric layers; in contrast, we found little to no relationship between FE and yarn diameter, fiber diameter, thread count, porosity, fabric thickness, and fabric material (e.g., natural vs. synthetic). Results of this work should help inform the design of more effective fabric masks, which could prove especially useful for airborne infectious disease response efforts in resource limited environments (i.e., where N95 technologies are not available) around the planet.

ACKNOWLEDGEMENTS

I would like to thank my advisor John Volckens for his consistent support and guidance during my time as a Master student and in the long process of realizing my thesis project. I'd also like to thank Christian L'Orange for providing invaluable support and resources in both the early stages of planning my thesis project and during the experimental and data collection stages of the project. I am grateful to Jack Kodros for his support in the writing of my thesis. His revisions of and feedback on my thesis document were very helpful.

I greatly appreciate Johns Volckens, Shantanu Jathar, and Ellison Carter for serving on my research committee and offering their time to review this thesis document.

Funding for this work was provided by the World Health Organization (2020/1073614-0).

TABLE OF CONTENTS

CHAPTER 1 – INTRODUCTION

1.1 Background

Since the emergence of COVID-19 and the ensuing pandemic, the use of face coverings has increased significantly among the global population [1, 2]. To be effective against infectious disease transmission, masks should offer two-way protection: filtration of inhaled air to protect the user, and filtration of exhaled air to protect the community [3]. In the occupational environment, surgical masks are intended to prevent the release of large droplets from the wearer (i.e., they provide community protection), whereas N95 Face-Filtering Respirators (FFRs), due to their ability to fit tightly over the face and efficiently filter particles across a range of sizes, can provide two-way protection [4]. The sudden need for face coverings offering two-way protection created a high demand for N95 FFRs in the early stages of the COVID-19 pandemic, ultimately resulting in a global shortage both in the public and in occupational settings [5]. Additionally, the Center for Disease Control (CDC) and the World Health Organization (WHO) actively advised the public against wearing N95 FFRs. Following this shortage of N95 FFRs and the reduced availability of surgical masks to the public, non-regulated masks made of fabric (i.e., material composed of woven or knit fibers) were often used by workers and members of the public; however, the effectiveness of these fabric masks at reducing exposure to particles with sizes relevant to the SARS-CoV-2 is not well understood. Further, fabric masks are available in a wide variety of materials (e.g., cotton, wool, polyester), of varying characteristics (e.g., thread count, yarn size, fiber diameter), and number of layers. To provide consistent guidelines on the design and use of fabric masks, understanding the relationship between fabric characteristics and mask performance is essential.

1.2 Defining basic terms

The performance of a mask or respirator is commonly quantified through the following metrics: filtration efficiency (FE), breathability, fit, and compliance. FE is a measure of a respiratory protective device's effectiveness at preventing particles from penetrating through the media (i.e., the ratio of particles

downstream to upstream of the material assuming all air passes through the material) [6]. The performance of a respiratory protective device is strongly linked to FE because the penetration of particles contributes to the inhaled dose, which is a major predictor of risk. The breathability of a respiratory protective device is characterized by its flow resistance, which is quantified by the pressure drop per unit face velocity through the device at a set flow rate. The fit of a device characterizes whether or not a device seals to the user's face. A tight seal limits the amount of airflow that bypasses the filter material and thus increases the amount of protection against infectious particles [6]. Compliance is a behavioral aspect related to the user and characterizes whether the user is following instructions and wearing the mask. Some major design parameters to optimize for higher probability of compliance include the comfort of fabric material, how the mask interfaces with the wearer's face (e.g., how the mask fastens to the ears, bridges the nose, forms to the cheekbone and jawbone, whether it remains in place or needs constant adjustment), and the microclimate (i.e., the temperature and humidity) in the mask during use. [7, 8].

1.3 Previous work

There is a growing body of literature evaluating the performance of fabric masks; however, methods among these initial studies are inconsistent. A common limitation is the particle size range chosen to evaluate FE. Many previous studies do not consider particle diameters larger than 1 μm [7, 8, 9, 10, 11, 12], which is potentially problematic because infectious SARS virions have been reported in sizes ranging from submicron to tens of microns in diameter (particle size is discussed in more detail later in this section) [13, 14]. Another common limitation is small sample size (i.e., small number of masks tested), with tests often considering fewer than ten fabrics [9, 10, 11, 13]. Finally, few studies have explored the relationship between fabric characteristics and mask FE–a necessary step to inform the design of improved respiratory protective devices.

Fabric masks commercially available to the public exhibit substantial variability in FE and tend to have notably lower FE than that of N95 respirators, surgical masks, and many common nonwoven masks across all measured particle sizes [8, 14]. Numerous studies have found that adding multiple fabric layers can substantially raise FE, though this comes at the cost of higher flow resistance [8, 10, 11, 14, 15].

Drewnick et al. (2021) also found that FE and flow resistance of the individual layers of a mask can be used to calculate the FE and flow resistance of the entire mask according to classical filtration theory [8, 16]. In contrast, Rogak et al. (2020) found that this calculation significantly overestimates FE for particle diameters between 1-3 μm, hypothesizing that some of the layers could be preferentially removing charged particles, though spun-bonded filters were considered in their analysis [9] Previous studies have found the particle size with the lowest efficiency (i.e., the MPPS – most penetrating particle size) to be between 0.3 to 0.5 μm for fabric masks [8, 14], whereas the MPPS for an N95 respirator made from electret fibers (i.e., fibers that are electrically charged to enhance the collection of submicron particles) around 0.05 μm or smaller [17].

The relationship between fabric mask characteristics and FE is unclear. Drewnick et al. (2021) found that thread count for woven fabrics is a poor predictor of FE. They hypothesize that fabrics with higher thread counts often feature thinner threads, thus reducing material thickness and reducing FE [8]. Conversely, Konda et al. (2021) found a strong positive correlation between thread count and FE [18], but their experimental methods have been scrutinized as flawed (e.g., particle sizes they considered are much smaller than those in the range of infectious SARS-CoV-2 particles). [21, 22, 23]. Drewnick et al. (2021) and Hao et al. (2021) found that FE increases with areal density of the fabric (i.e., cloth cover factor), while Mirrielees et al. (2021) found no correlation between pore size (a direct corollary of cloth cover factor) and FE [7, 8, 11]. Additionally, Hao et al. (2021) reported that fabric porosity had a slight negative correlation with FE. Rogak et al. (2021) hypothesized that the more napped fabrics (i.e., fabrics with frayed fibers, "fuzzy") served as better filters. This hypothesis was based on the examination of higher performing fabrics under an optical microscope [14].

1.4 Knowledge gaps

There is currently limited understanding of the associated between common fabric characteristics and the performance of a fabric masks. The characteristics of fabrics defined and used by the textile industry (e.g., thread count, cloth cover factor, porosity) primarily exist to communicate industry-specific measures,

such as comfort, material strength, elasticity, and absorbency. It is unclear whether these characteristics have any association with a fabric mask's ability to filter airborne particles. Understanding the relationship between the performance of a fabric mask and its characteristics as defined in the textile industry would enable commercial manufacturers, as well as the public, to interpret and apply this information for designing and choosing the most effective masks and materials.

1.5 Objectives

This work explores the relationship between the characteristics of a fabric mask and FE to inform the design of effective fabric masks used for personal protection. In Section 2, we detail our methods for measuring FE of all 50 masks and 70 component fabric layers, flow resistance of all masks/layers, and the characteristics of each fabric layer. Eight characteristics were evaluated for each fabric, namely, thread count, yarn diameter, fiber diameter, porosity (ratio of free space to fiber material), air permeability, cloth cover factor (a proportion of the fabric area covered by yarn), IR attenuation (reduction in intensity of IR light across a fabric material), and fabric thickness. Our working hypothesis is that none of the fabric characteristics examined in this study are correlated with FE and flow resistance. In Section 3, we present all FE and flow resistance data, exploring the relationship between FE, flow resistance, and fabric characteristics. Finally, in Section 4 we discuss our conclusions, study limitations, and opportunities for future work.

CHAPTER 2 – METHODS

2.1 Filtration Efficiency (FE)

Fifty commonly worn fabric masks commercially available to the public were collected from a group of volunteers in Fort Collins, Colorado, as part of an unrelated study investigating aerosol emissions from vocalization [19]. Following a similar procedure to that presented in Leith et al. (2021), the FE and flow resistance were evaluated by testing each mask in an aerosol chamber, before separating the individual layers of each mask and following the same procedure for all 70 fabric layers [6]. The procedure for testing FE and flow resistance is briefly described here (Figure 1). Each mask was secured to one end of a cylinder with an 89 mm inside diameter by a ring clamp. This diameter was chosen to be representative of the area that air passes through when a mask is worn. A second, identical cylinder without a mask attached was used to measure background particle concentrations within the chamber. Either cylinder could be placed at the top of a vertical sampling column in a 0.7 m^3 aerosol chamber. Chamber air was pulled through a sampling column at 15 L min^{-1} by a vacuum pump. This flow rate roughly represents that of inhalation and exhalation when not speaking [6]. The sampling column (2" inner diameter, 11" in height) was sized to ensure isokinetic sampling. To model exhalation, the masks were mounted backwards onto the cylinder so that the flow entered through the back of the mask, though the orientation of the mask should not have a significant impact on FE [6].

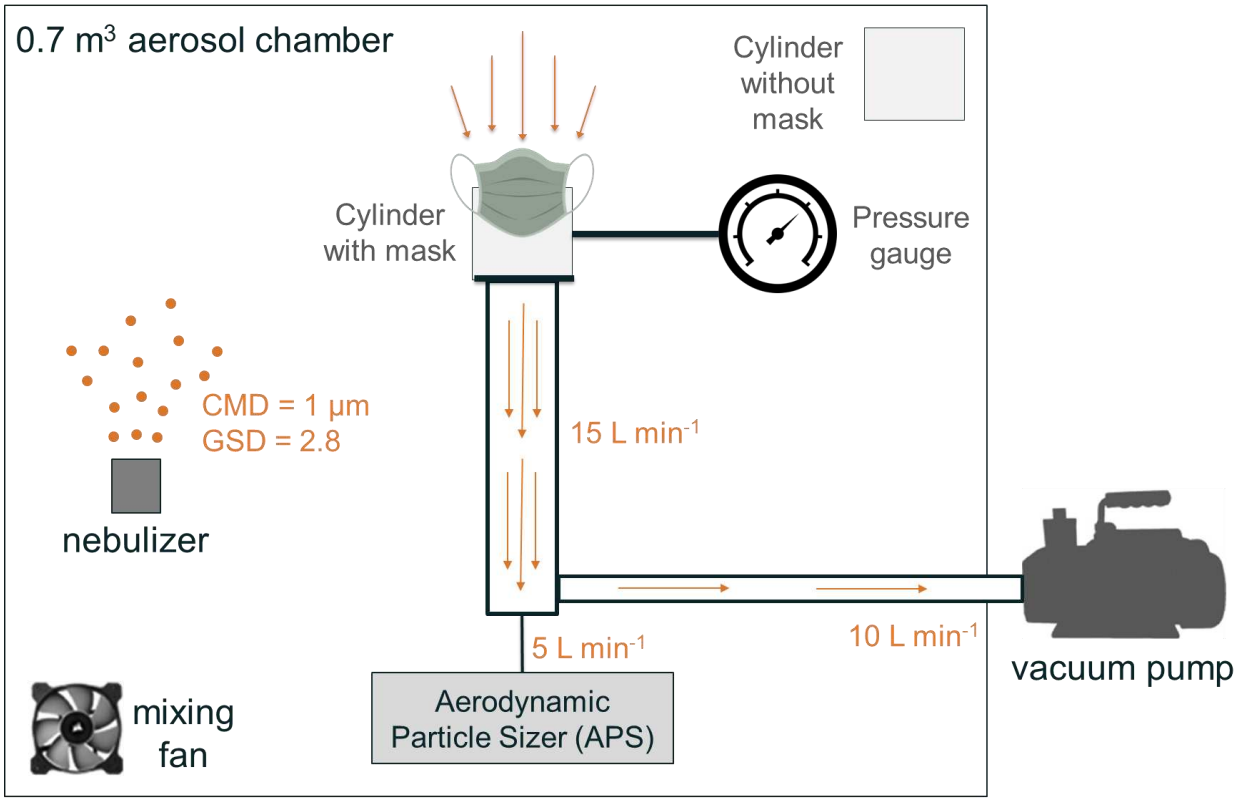

Figure 1: Schematic of experimental setup

At the bottom of the sampling column, an upwards facing, axially aligned probe led to an aerodynamic particle sizer (APS Model 3321, TSI Inc. Shoreview MN) that sampled column air at 5 L min^{-1}**.** The APS in this configuration is capable of measuring 42 size bins with aerodynamic particle sizes ranging from 0.5 to 20 µm. Excess air left through a T below the sampling probe, passing through the vacuum pump. A nebulizer (Micro Mist 1880, Hudson Respiratory Care Inc. Temecula, CA) in the chamber generated polydisperse droplets of non-volatile compressor oil with density 0.867 g cm^{-3} (Ace Hardware Corp., Oak Brook IL).

Particle concentrations in the aerosol chamber were measured over two separate, two-minute intervals– the first interval with the mask attached to the sampling column and the second interval without the mask attached (to measure background concentrations). At least one minute elapsed between measurements to allow particle concentrations within the chamber to stabilize. This process was repeated until six paired

samples were measured. The FE was calculated from the particle concentrations measured with and without the mask attached to the sampling column following Equation 1,

$$\eta(d) = 1 - \frac{C_{on}}{C_{off}} , \qquad (1)$$

where η(d) represents FE as a function of particle diameter, "C_{on}" represents particle number penetrating the mask, and "C_{off}" represents the background particle number. At least two FE tests were completed for each mask (i.e., at least 12 tests in total). This experimental design in which sample pairs are created just one minute apart helps eliminate measurement error due to particle concentration drift in the chamber. To minimize coincidence errors (i.e., particle counting errors that begin to occur when concentrations are above 1000 cm^{-3}) in the APS, particle concentrations within the chamber were kept below about 40 cm^{-3}. Because of the low particle concentration used for testing, the effect of particle loading on the masks was not considered in this study. Additionally, these masks are most often worn in relatively "clean" environments (e.g., the home, indoor office, grocery store, gym), not dusty environments where particle loading would begin to take effect. The masks were tested using a specific aerosol with a specific size distribution in this study. However, due to the APS being highly linear across particle concentrations and size distributions, the resulting particle counts (and thus FE) from our testing can be extrapolated to different aerosols with different size distributions.

In addition to FE, we evaluated the flow resistance of each mask. A Magnihelic gauge (Dwyer, Michigan City IN) measured pressure drop across each mask while attached to the sampling column (and so represents pressure drop at a flow rate of 15 L min^{-1}). To calculate flow resistance, the pressure drop was divided by the face velocity incident on the mask.

Finally, we separated the mask into its component layers and repeated the same procedure to measure the FE and pressure drop (and thus evaluated flow resistance) of the individual layers. We tested a total of 70 layers across all masks. The FE and flow resistance data from each layer were used for comparison against the layer's characteristics.

2.2 Fabric Characteristics

Below, the methods for deriving the following fabric characteristics are explained: thread count, yarn diameter, fiber diameter, porosity, air permeability, cloth cover factor, IR attenuation, and fabric thickness. A 2-inch circular sample cut from each fabric layer was examined under an optical microscope (ORTHOPLAN, Leitz) to determine the fabric's characteristics. Images of the layers were taken using a camera (GRYPHAX NAOS, JENOPTIK) integrated into the microscope. Yarn diameter, fiber diameter, and thread count for each fabric were all measured directly from the images using tools within the camera's software (GRYPHAX, JENOPTIK). Measurements were taken at least 2 mm away from the outside edge of the cut sample to eliminate errors due to any warping of the fabric. The yarn diameter and thread count data were used to calculate the cloth cover factor of the fabric (i.e., the fraction of the fabric's projected area covered by yarn).

Yarn diameter was measured as shown in Figure 2A. For woven fabrics, 10 total measurements were taken, 5 from vertical threads and 5 from horizontal threads ("vertical" and "horizontal" relative to the microscope image taken). The measurements of yarn diameter for vertical and horizontal threads were taken separately because, for some layers, the vertical and horizontal threads were consistently differently sized. Measured diameters from the vertical and horizontal threads were averaged to give a representative yarn diameter to be used for the data analysis. For knit fabrics, 10 measurements were taken and averaged. For both knit and woven fabrics, each measurement was taken from a unique yarn at various spatially distributed points throughout the sample.

Fiber diameter was measured as shown in Figure 2B. Ten measurements were taken at various spatially distributed points throughout the layer sample. Natural fibers have a ribbon-like shape and often vary in size, making it difficult to determine an accurate representative fiber diameter for the fabric (Figure 2). Mirrielees et al. (2021) also reported methodological challenges when characterizing fiber diameter [11]. Therefore, the natural fiber diameters presented in this work are only those that were measured with minimal variability across the ten measurements taken. In contrast, for synthetic fibers like polyester or

spandex, fiber diameter for the fabric is reported as an average of 10 measurements due to the fibers' uniform cross section and size throughout the sample.

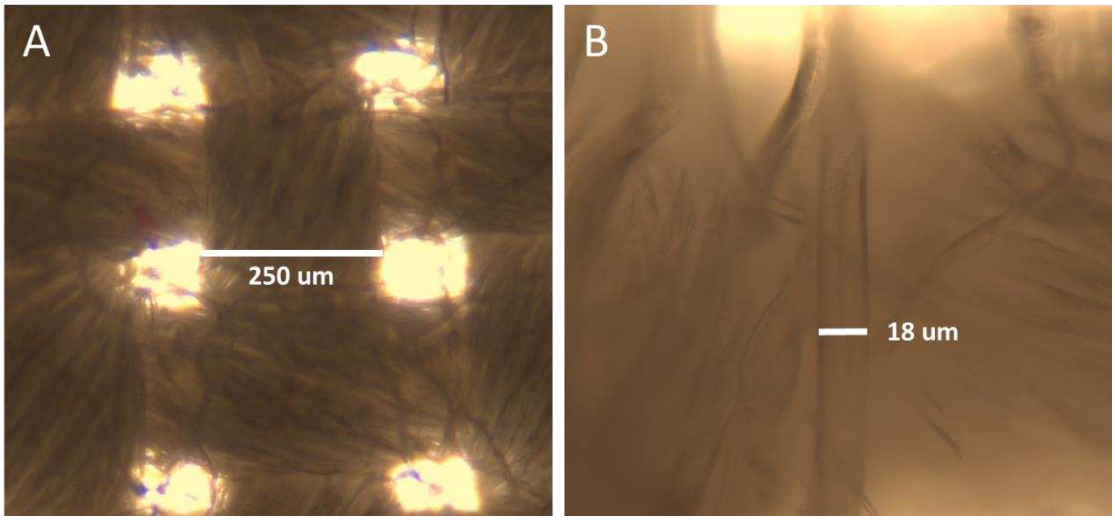

Figure 2. Optical measurement of yarn diameter (A) and fiber diameter (B). The fabric shown contains natural fibers.

Thread count was measured using Equation 2 and as shown in Figure 3. For woven fabrics, the maximum number of weft and warp threads within the microscope's field-of-view were counted to obtain the thread count for the fabric. Preliminary tests showed that measuring thread count using a single microscope image produced an accurate measure of thread count for the entire fabric (i.e., the thread count measured across a large sample of fabric was the same as that measured from a microscope image). The counts were divided by the distance over which they were taken and summed to calculate thread count. The same procedure was followed for counting the courses (i.e., crosswise rows of loops) and wales (i.e., columns of loops running lengthwise) to obtain thread count for knit fabrics.

$$\mathrm{TPI}_{\mathrm{woven}} = \left(25.4\frac{\mathrm{mm}}{\mathrm{inch}}\right)\left(\frac{\text{vertical threads}}{\mathrm{mm}} + \frac{\text{horizontal threads}}{\mathrm{mm}}\right) \tag{2}$$

$$\mathrm{TPI}_{\mathrm{knit}} = \left(25.4\frac{\mathrm{mm}}{\mathrm{inch}}\right)\left(\frac{\text{wales}}{\mathrm{mm}} + \frac{\text{courses}}{\mathrm{mm}}\right)$$

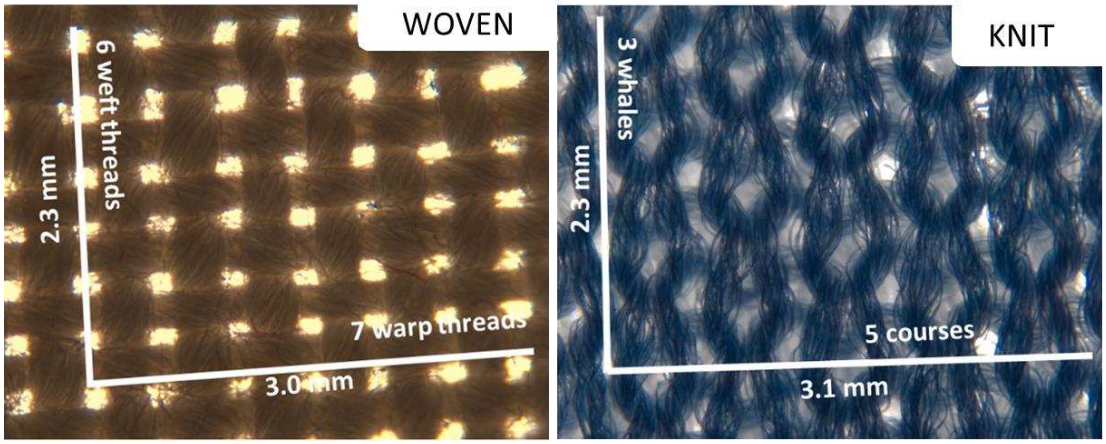

Figure 3. Optical measurement of thread count for woven and knit fabrics.

Each circular fabric sample was weighed using a Veritas M124A analytical balance (HOGENTOGLER, Columba MD). Fabric thickness was measured using a Digimatic Digital Thickness Gauge (Mitutoyo, Takatsu-ku Kawasaki Kanagawa) according to ASTM standard D1777 − 96. Both the weight and thickness of the fabric sample were used to calculate the volumetric porosity of the fabric to be used later in analysis.

2.3 IR attenuation

Circular samples 25 mm in diameter were cut from each layer and placed inside an optical transmissometer (Sootscan Model OT21, Magee Scientific) to measure their attenuation of infra-red (IR) light ($\lambda = 780$ nm to 1 mm). From the attenuation data, IR attenuation was calculated for each fabric layer. Preliminary tests showed that the transmittance of fabrics under ultra-violet light ($\lambda =$ 100 to 400 nm) and visible light ($\lambda = 380$ to 700 nm) was not associated with fabric FE or flow resistance. The type of fabric dye present in the sample, and possibly the fabric material itself (e.g., cotton, wool, polyester, etc.), affected the fabric's transmittance of UV and visible light. IR attenuation was shown to be relatively independent of fabric dye and material.

2.4 Data Analyses

In this section, the methods used for analyzing the data resulting from both the FE testing and all fabric characterization are summarized. All data analyses were conducted in R (R Core Team, version 4.1.2). Average values, standard deviations, or ranges (when appropriate) were calculated for all fabric

characteristics, flow resistance, and FE measures for all 70 fabric layers. Relationships between fabric characteristics, FE, and flow resistance were evaluated using Spearman correlations and simple linear models. The goal in using these linear models was to determine whether or not the characteristics of a fabric have any association with its performance. Using the coefficients from the linear regression outputs, linear fit lines were created and included on all relevant plots. Tables containing statistics related to all linear models–namely the estimate, standard error, F-statistic, p value, and confidence interval–are included in Table 1. A Welch two sample t-test was performed to compare the means in FE between natural and synthetic layers. To visualize the relationship between FE and particle diameter for all masks and their component layers, a three-parameter nonlinear regression was used to create smooth curves from the raw FE data [6]. Transforming the FE data points into smooth curves for the masks and layers made visualizing the FE distributions easier.

CHAPTER 3 – RESULTS

3.1 Filtration Efficiency as a function of particle diameter

3.1.1 *Mask FE*

To test the effectiveness of cloth masks, we measured the FE of 50 masks as a function of particle diameter. The aerosol used for testing had a count median diameter of 1 µm and a geometric standard deviation of 2.8. Across all masks, with the exception of the three containing filters, FE was relatively low (average of 32% and range between 10% and 69% at 720 nm) for submicron particles but rose to higher values (average of 81% and range between 48% and 100% at 5 µm) with increasing particle diameter (Figure 4). The scattered FE data was transformed into smooth lines as shown in Figure 4 using a three-parameter nonlinear regression. The scattered data (without the regression applied) is shown for reference in Figure 17. Here, FE was highest at the largest particle diameter measured, 12 µm, and lowest at the lowest particle diameter measured, 0.5 µm. This FE distribution across particle diameter is expected according to aerosol theory. Because of the large threads and relatively large pore sizes, interception and inertial impaction are likely the dominant particle collection mechanisms, with larger particles striking the fibers and threads directly, whereas diffusion and settling are less prominent, with smaller particles following the streamlines directly through the open pores [16]. The masks that did not contain a filter had FEs between 8% and 60% at submicron particle diameters. Nearly half the masks in the set (21 out of 50 masks) did not meet the Level 1 barrier standard (20% minimum FE in the submicron range) specified in ASTM F3502-21 (Figure 13). Nine of the masks (including the three containing filters) met the Level 2 barrier standard (50% minimum FE in the submicron range). The ASTM F3502-21 standard serves to ensure masks provide two-way protection (i.e., they reduce expelled droplets and aerosols from the wearer and offer particle filtration to reduce the amount of inhaled particle matter by the wearer). Therefore, according to this standard, 21 masks in this set do not offer sufficient protection to the wearer, 20 masks offer “minimal” protection, and 9 masks offer “good” protection.

For comparison, the FE of an N95 FFR is shown in red in Figure 4. The N95 FFR had the highest FE of the masks tested here, with a minimum FE of 99% across the range of particle diameters tested. The three masks with an interior filter performed notably better than all fabric masks without a filter, with an average submicron FE of 93%.

In agreement with our findings, Kwong et al., 2021, in a review on previous work studying the performance of common materials used for face masks, found similar FEs for single and multilayered fabric masks and demonstrated the large difference in FE between fabrics and N95 FFRs [20]. The FE of fabrics have previously been shown to be lowest between ~0.3 μm to ~0.6 μm, which is consistent with our findings [8, 20, 21].

The vertical line shown in Figure 3 represents a diameter of 2.0 μm, which is the particle diameter where the largest variation in FE occurs in the mask set. Across the cloth masks tested, FE ranged from 22% to 90% at this particle diameter. Differences between masks characteristics appear to affect performance most prominently at this size; additionally, as discussed in the previous section, SARS-CoV-2 has been shown to be infectious in this size range.

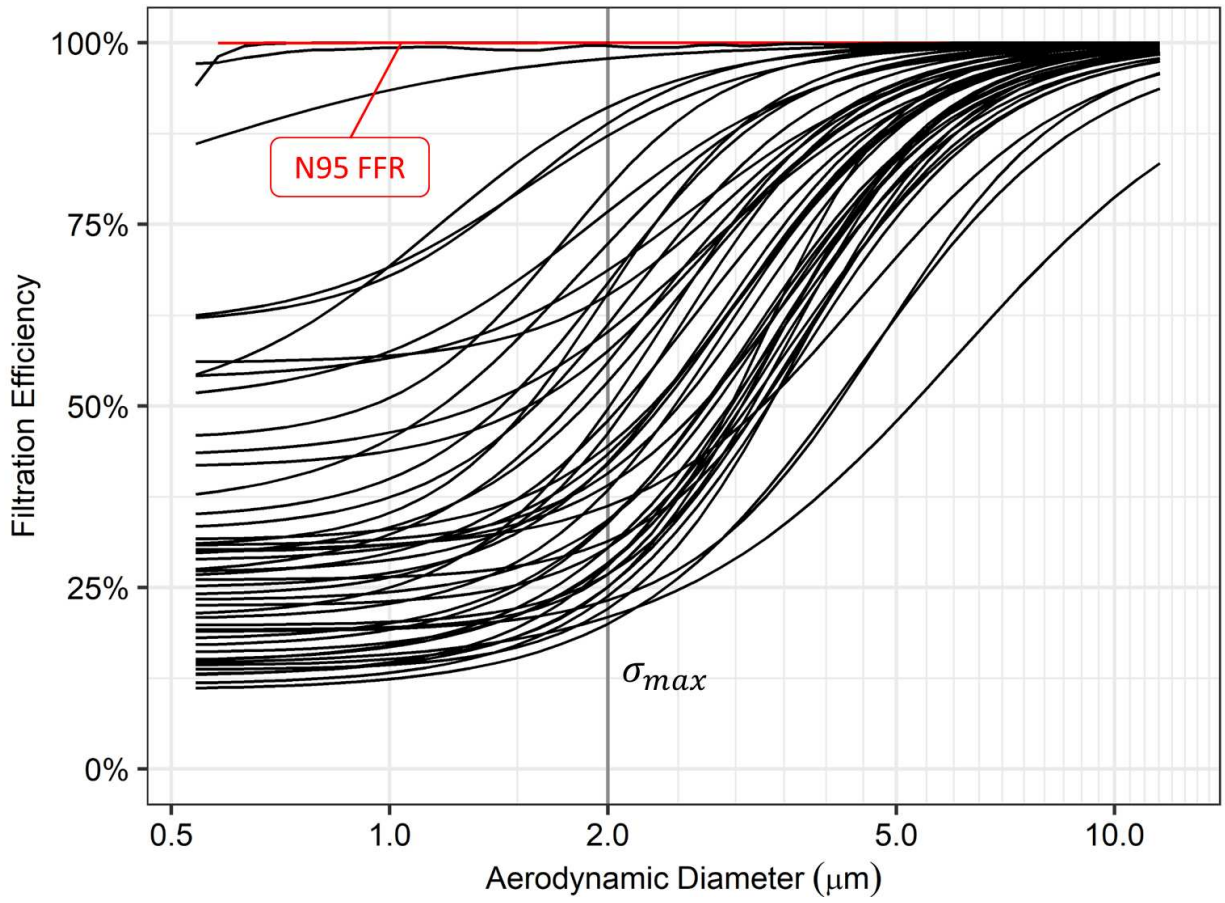

Figure 4: Filtration Efficiency (FE) for 50 fabric masks. The FE of an N95 FFR is shown in red. The highest variation in FE in the mask set, σ_{max} , was recorded at 2.0 μm.

3.1.2. *Predicting Mask FE*

We measured the FE of the component layers for each mask individually to test the relationship between total mask FE and that of the component layers. We found that FE of a mask can be predicted by the FE of its component layers to within 11% accuracy (Figure 5). At a particle diameter of 2 μm, the coefficient of determination (r^2) between the measured FE and the predicted FE was 0.81. Therefore, fabric masks can be generally treated as filters in series in terms of FE, in agreement with previous findings [8].

Further, we compared the predicted and measured FE of cloth masks composed of two layers against those of three layers (Figure 5). We found that our model has a slightly higher mean absolute error for masks composed of three layers (ranging from 1-11% across particle diameters) than for those composed of two layers (ranging from 2-5% across all measured particle diameters). This finding implies that this

prediction could be less accurate for masks made of many layers. Future studies can explore the effect of layering on this prediction.

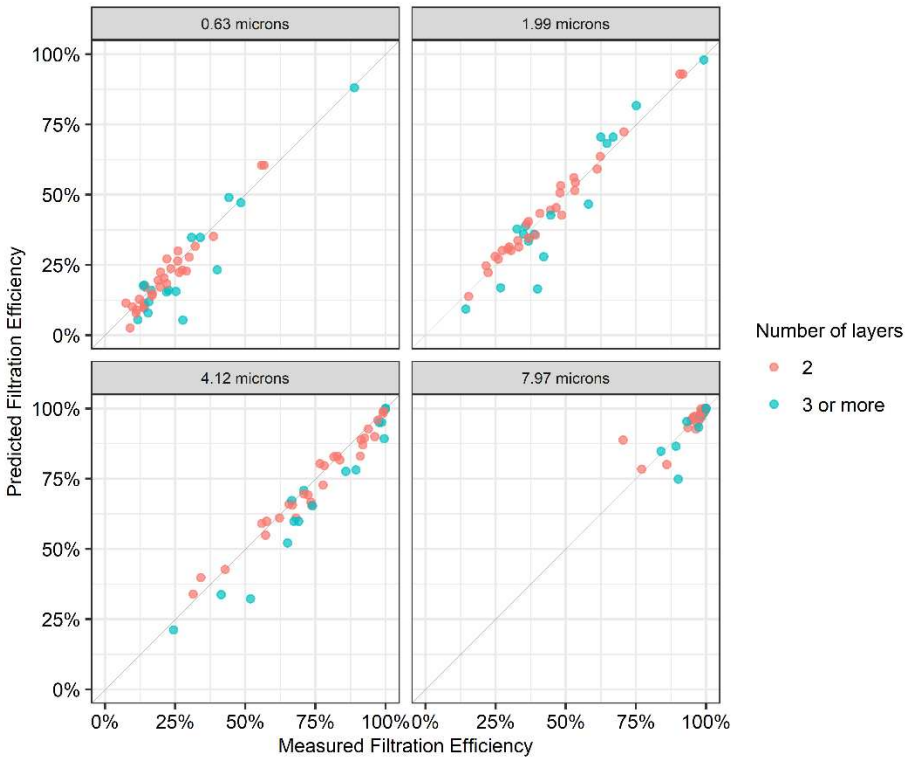

Figure 5: Comparing the FE measured from each mask (x-axis) to the FE predicted for each mask using the FE from its component layers (y-axis). The diagonal line, y=x, represents perfect agreement between the measured FE and the predicted FE.

3.1.3 *Layer FE*

Measurements of FE for individual layers are shown in Figure 6 for natural and synthetic materials (excluding the three filter insert layers). As expected, the FE of the individual layers is lower than that for the entire mask while retaining the same characteristic dependence on particle diameter (Figure 6). All mask layers with the exception of two had FEs less than 25% at the MPPS. Across the fabric layers considered here, we found no notable differences in FE between natural and synthetic layers ($p = 0.72$).

We measured several outliers in our measurement set that had higher than average FE (layers labeled as A, B, and C in Figure 6) and lower than average FE (layers labeled D, E, and F in Figure 6). Images of these layers are shown in Figure 7. The higher performing layers are tightly knit and woven, with notably smaller pores than the lower performing layers.

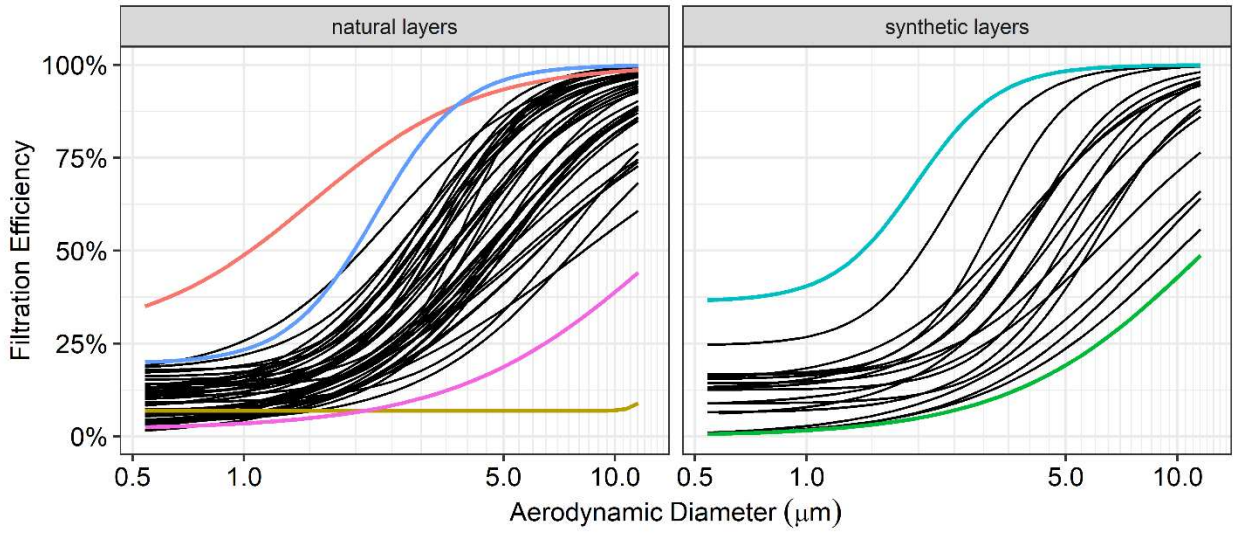

Figure 6: The Filtration Efficiency (FE) of 70 individual fabric layers as a function of particle diameter for (left) natural fabrics and (right) synthetic fabrics. Highlighted measurements, A, B, and C, represent the best performing layers, while D, E, and F represent the worst.

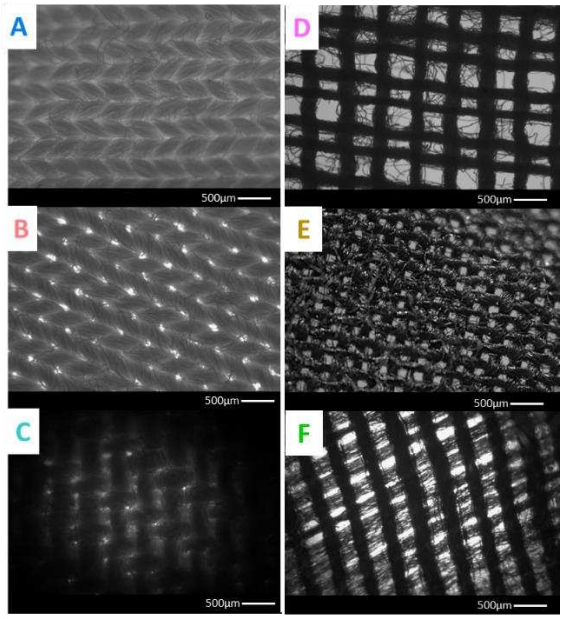

Figure 7: Microscope images of the fabric layers with the (A-C) highest FE and the (D-F) lowest FE. Fabrics A, B, C, D, E, and F had the following FEs at 2 μm, respectively: 49%, 73%, 64%, 5%, 3%, 4%.

3.2 FE and fabric characteristics

3.2.1 *Flow resistance*

We evaluated fabric flow resistance across all 70 layers and compared them to the FEs of the layers. Flow resistance affects the breathability of a mask, a major contributor to mask wearability. Masks with higher flow resistance perform better but are less breathable and therefore wearable. Across all layers considered here, the flow resistance ranged from 2.0 – 38.6 mm H_2O L^{-1} s. As expected, we found that FE increases with increasing flow resistance across a fabric layer (Figure 7). This increase is nonlinear, which is consistent with previous studies [11, 14]. Additionally, the relationship between FE and flow resistance depends on particle diameter.

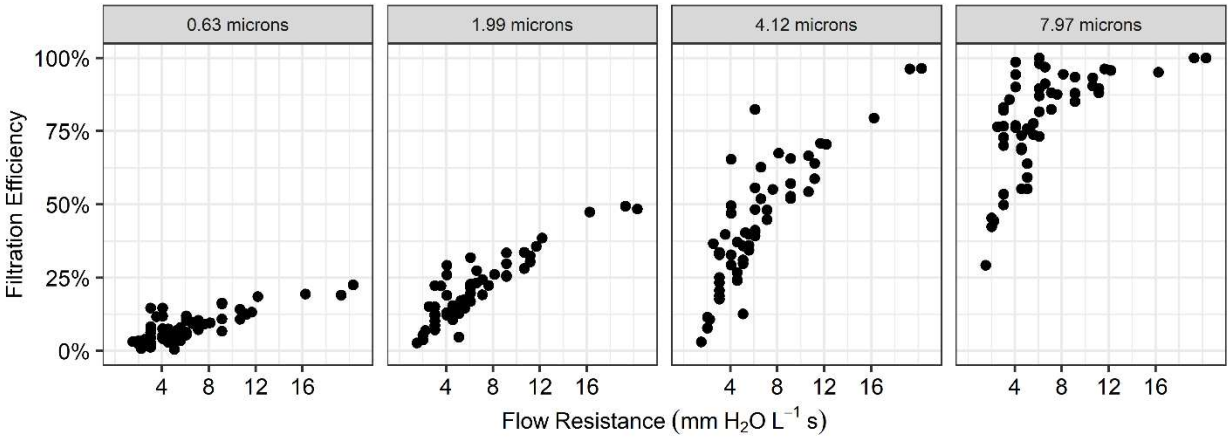

Figure 8: Filtration efficiency (FE) at particle diameters of (a) 0.63, (b) 1.99, (c) 4.12, and (d) 7.97 µm plotted against flow resistance for each fabric layer.

Cumulative distribution function plots for all eight fabric characteristics studied are presented in Figure 18. We explored how flow resistance relates to several commonly used fabric characteristics. Cloth cover factor and air permeability were strongly correlated with flow resistance (ρ = 0.61 and 0.89, respectively) (Figure 9). Porosity was weakly correlated with flow resistance (ρ = 0.28). In contrast, thread count, fiber diameter, and yarn diameter had no association with flow resistance.

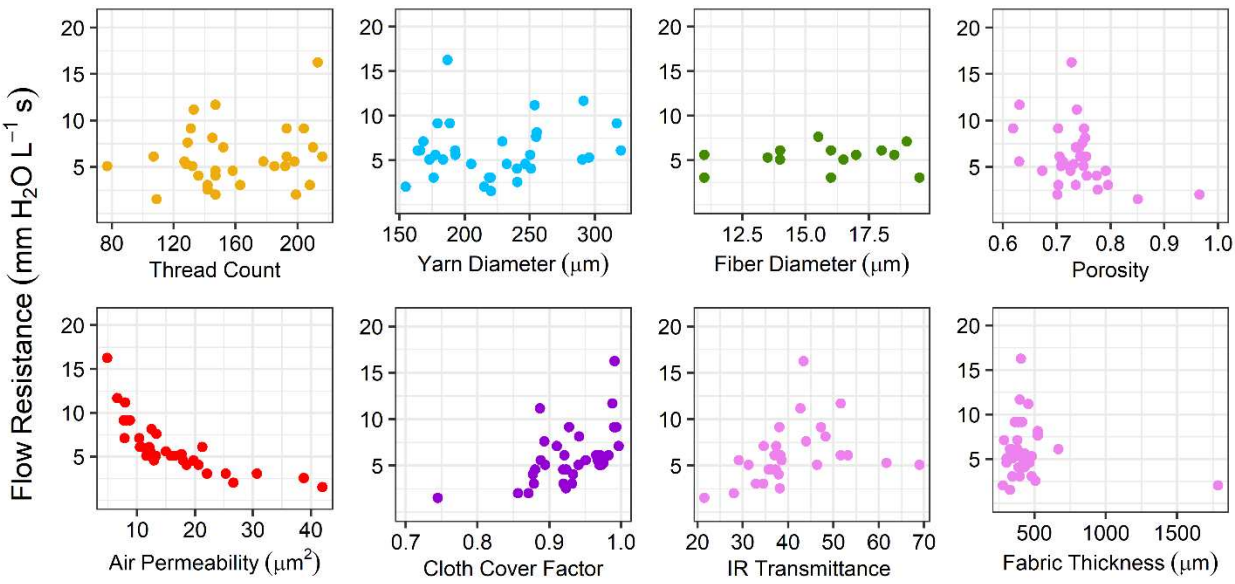

Figure 9: The association between flow resistance and (a) thread count, (b) yarn diameter, (c) fiber diameter, (d) porosity, (e) air permeability, (f) cloth cover factor, (g) IR attenuation, and (h), fabric thickness

3.2.2. *Filtration Efficiency (FE)*

We explored the relationship between FE of individual layers with thread count, yarn diameter, fiber diameter, porosity, air permeability, cloth cover factor, IR attenuation, and fabric thickness (Figure 10). We quantified this relationship with a linear model and found a moderate relationship between FE and cloth cover factor (ρ = 0.51, 0.60, 0.59, and 0.53 at diameters 0.63, 1.99, 4.12, and 7.97 μm, respectively) , IR attenuation (ρ = 0.48, 0.51, 0.58, and 0.58), and air permeability (ρ = 0.53, 0.64, 0.64, and 0.46); however, we found little to no relationship between FE and yarn diameter, fiber diameter, thread count, and porosity.

.

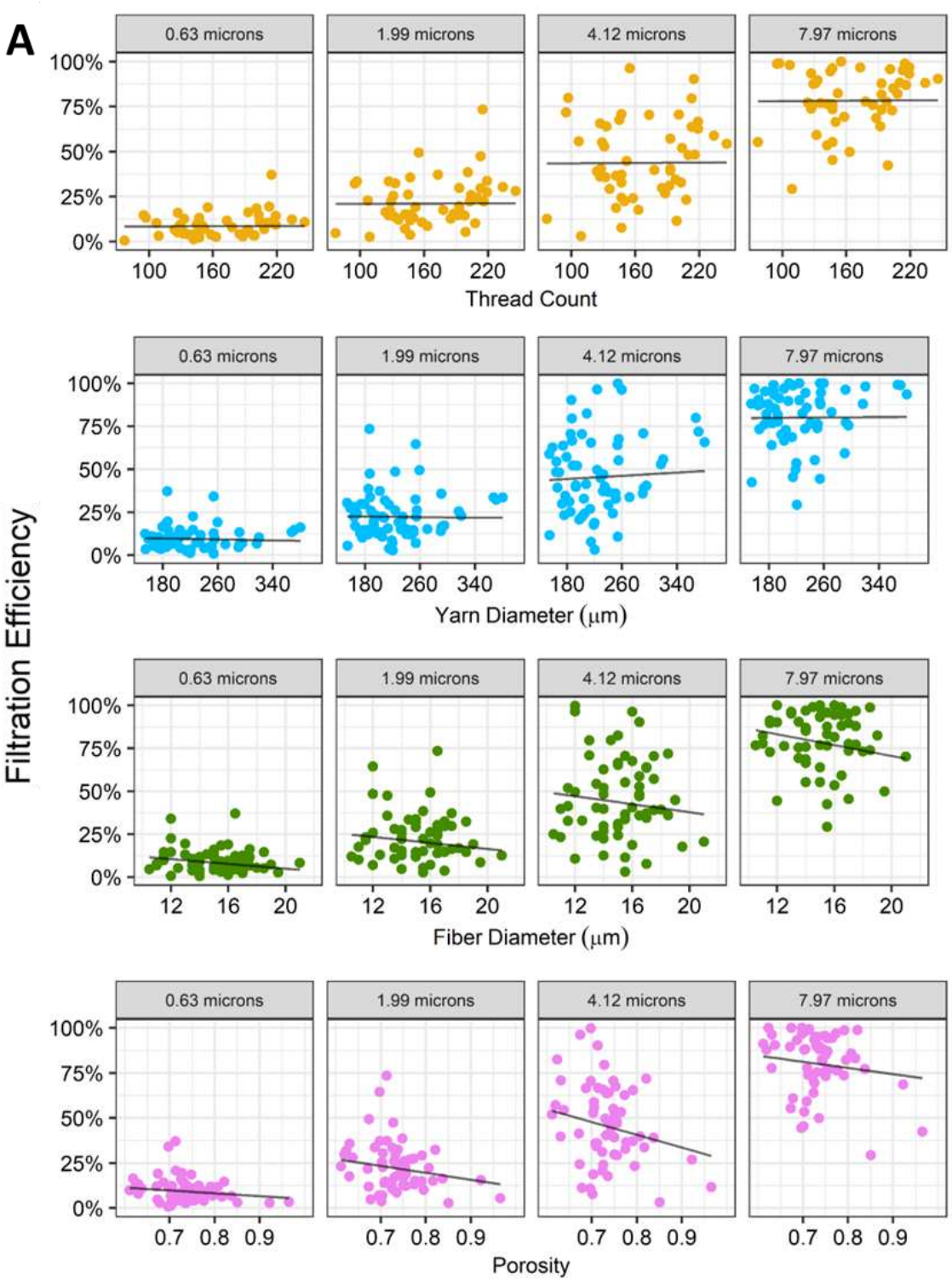
A
0.63 microns
1.99 microns
4.12 microns
7.97 microns
Filtration Efficiency
100%
75%
50%
25%
0%
100 160 220
Thread Count
180 260 340
Yarn Diameter (μm)
12 16 20
Fiber Diameter (μm)
0.7 0.8 0.9
Porosity

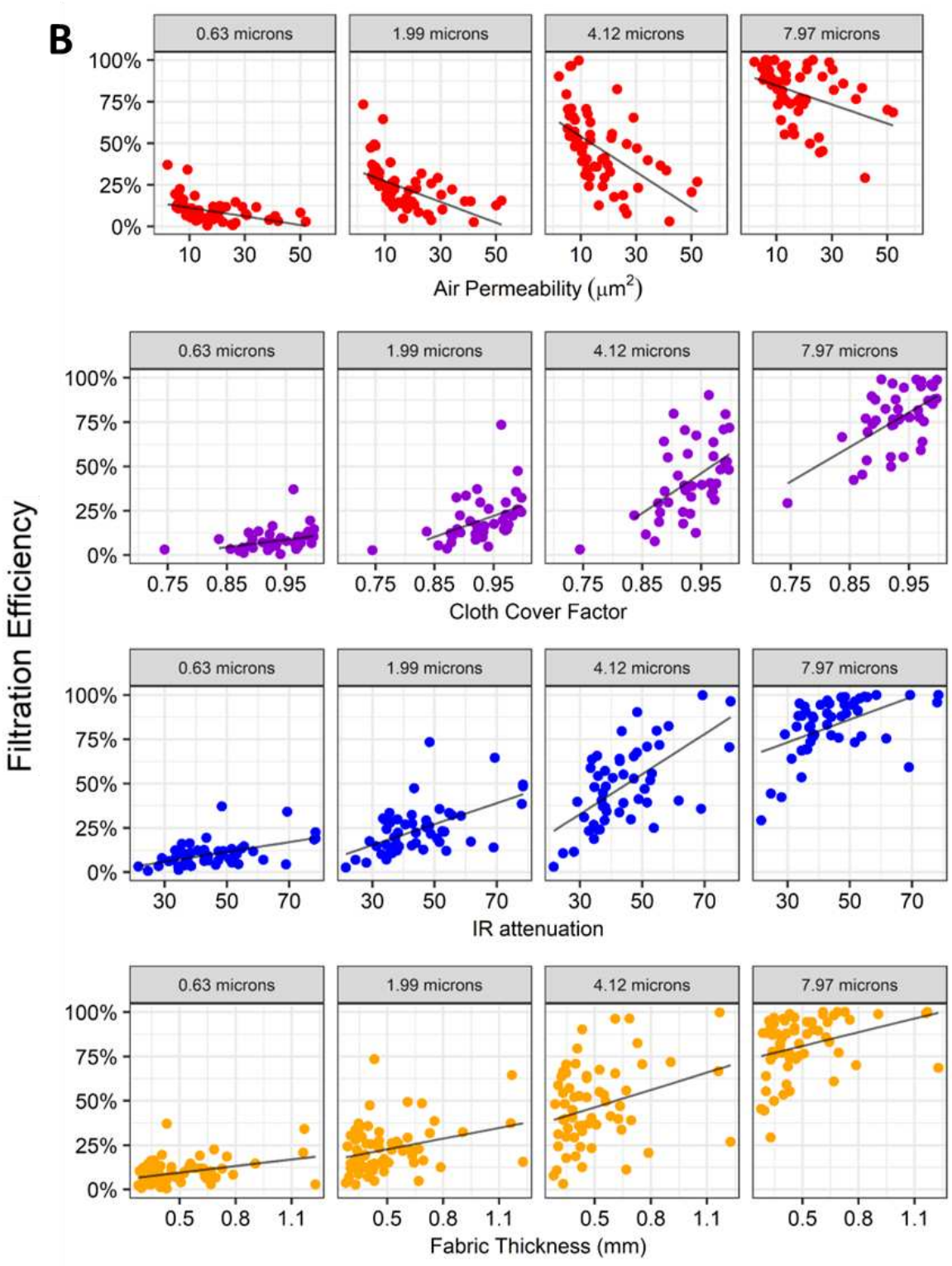

Figure 10A, 10B: Filtration efficiency (FE) for all 70 layers at 4 different particle diameters plotted against the following fabric characteristics: thread count (orange), yarn diameter (light blue), fiber diameter (green), porosity (light purple), air permeability (red), cloth cover factor (purple), IR attenuation (blue), and fabric thickness (dark orange). A linear regression line is shown on each plot.

CHAPTER 4 – DISCUSSION AND CONCLUSIONS

The FE of fabric masks was relatively low for particles with diameters in the submicron size range (average of 32% and range between 10% and 69% at 720 nm) but was higher for particles with diameters greater than a micron (average of 81% and range between 48% and 100% at 5 μm). This behavior follows traditional aerosol filtration theory, where interception and inertial impaction are likely the dominant particle collection mechanisms, and diffusion and settling are less prominent. Traditional aerosol filtration theory also suggests that a plot of FE vs. particle diameter should give rise to a characteristic "S" shaped curve which results from the combined effect of the single-fiber collection mechanisms (i.e., settling, impaction, diffusion, interception, and electrostatics), as shown in Figure 5. This set of fabric masks performed notably worse than a typical N95 FFR (minimum FE of 99% across all particle sizes tested), with 42% of the masks not meeting the Level 1 barrier standard (20% minimum FE in the submicron range) specified in ASTM F3502-21. Thus, our results confirm published guidance from public health agencies that fabric masks offer reduced protection from exposure to submicron aerosol [24]. The largest variation in FE in the mask set was found at a particle size of 2.0 μm. Therefore, for FE testing of masks for the public (assuming a resting breathing rate of 15 L min^{-1}), we recommend 2.0 μm aerodynamic diameter as the primary size of interest.

Overall, we found the flow resistance in the set of masks to be mostly at or below recommended values, with 38 of the 50 masks meeting the NIOSH maximum standard of 15 $mm\ H_2O\ L^{-1}$ s. Flow resistance exhibited a positive, nonlinear relationship with FE and was stronger with increasing particle size. From Figure 13, 76% of masks met the NIOSH criteria, indicating that most of these masks are highly breathable. However, breathability and FE are often indirectly related, as shown in Figure 9.

We investigated the dependence of FE of fabric masks on the FE of its component layers, flow resistance through the layers, and fabric characteristics, with all layers but two having FEs less than 25% at the most penetrating particle size (MPPS). FE was not significantly different between layers made of

natural and synthetic fibers ($p = 0.72$). We found that the FE of the component mask layers was a good predictor of the overall FE of the mask (mean absolute error ranging from 1-11%). This finding means that, as long as the FE the component layers are known (the layers can be different in characteristics), the FE of the mask can be immediately predicted, thus avoiding costly mask FE testing. Additionally, the flow resistance of the masks can be predicted by the flow resistance of the component layers (mean absolute error of 2.28 $\text{mm } H_2O \text{ L}^{-1} \text{ s}$). However, we found a small yet consistent overprediction. We hypothesize that this difference is due to the fact that entry losses between multiple mask layers are reduced for airflow exiting one mask layer and entering the next. Thus, given that the FE and flow resistance can be predicted well according to aerosol filtration theory, layered masks can generally be treated as filters in series.

To understand how the characteristics of a mask relate to its performance, we imaged the component fabric layers using an optical microscope and measured yarn diameter, fiber diameter, and thread count. Additionally, we measured the fabric attenuation to IR light using a spectrometer and fabric thickness using a thickness gauge. From these measurements, we derived the cloth cover factor, porosity, air permeability, and IR attenuation of the fabrics. Using a linear model, we found a moderate relationship between FE and cloth cover factor, IR attenuation, and air permeability; however, we found little to no relationship between FE and yarn diameter, fiber diameter, thread count, porosity, and fabric thickness. The finding that thread count is not a was not associated with FE is notable given the common conception during the early stages of the pandemic that higher thread count fabrics ensured better protection than lower thread count fabrics. Given that IR attenuation does exhibit an association with FE, IR spectrometry could serve as an alternative FE testing method for expensive and time-consuming traditional testing methods.

In the following paragraphs, we make recommendations for best practices regarding the design of fabric face coverings. Our results indicate that the fabric material of the fabric is not a determinant of FE: synthetic fibers (e.g., polyester, polypropylene) and natural fibers (e.g., cotton, flax, silk) perform similarly. By themselves, thread count, fiber diameter, and yarn diameter do not seem to be associated with performance; however, cloth cover factor, which is a function of these three characteristics, is associated with performance. Fabric with high cloth cover factor feature small pores, thus increasing the

surface area for particles (especially larger particles) to contact with the fibers/threads directly. Therefore, the cloth cover factor (i.e., the fraction of the area of fabric covered by yarn) of a fabric should be maximized for higher performance while considering the resulting decrease in breathability.

Adding multiple layers to a mask can substantially increase mask FE at the cost of lower breathability. With each added layer, mask FE increases asymptotically (i.e., adding layers has diminishing returns on FE), while the flow resistance, and therefore breathability, increases additively. In other words, flow resistance increases proportionally more than FE increases when adding multiple layers.

There are several important limitations in this study. The first is that the masks tested had potentially experienced some wear, as they were collected from a group of volunteers that had likely worn the masks previously (the duration of which was unknown). However, the fabric characterization methods used in this study were carefully designed such that any wear or loss of function should have been reflected in a change of material property (e.g., cloth cover factor, flow resistance). The results reported here apply only to masks made of fabric–not high efficiency for-purpose PPE or respirators. However, our results are pertinent to those living or working in resource limited environments, where N95 respirators are not readily available. We tested a limited range of particle sizes (0.5 to ~10 μm) and did not evaluate FE for large particles/droplets or for particles smaller than 0.5 μm. Considering, however, that our data followed aerosol filtration theory, FE at particle sizes smaller than 0.5 μm could be predicted using our data and FE at particle sizes larger than 10 μm are expected to approach unity. Lastly, while the FE we report represents the inherent performance of a mask, the actual performance of a mask while being worn is largely dependent on the fit of the mask to the wearer's face. Any leakage of air around the mask can substantially reduce the number of particles filtered by the mask. The strengths of this study include the following: the large sample size of 50 masks tested and 70 layers characterized, the selection of masks representative of those commonly worn by the public, the use of established methods for measuring FE

and flow resistance, and the testing of particle sizes in a relevant size range for airborne transmission of SARS-CoV-2.

There are numerous opportunities for future work regarding the performance of fabric masks. Along with interception and inertial impaction, electrostatic collection is could be a major contributor to the collection of particles in fabric masks. Future work can explore the association between this and FE. Previous work has explored how FE varies with breathing rate; however, the dependence of breathing rate on the FE-fabric characteristic relationship is unknown.

CHAPTER 5 – REFERENCES

1. Cheng, V. C.-C., Wong, S.-C., Chuang, V. W.-M., So, S. Y.-C., Chen, J. H.-K., Sridhar, S., et al., *The role of community-wide wearing of face mask for control of coronavirus disease 2019 (COVID-19) epidemic due to SARS-CoV-2*. The Journal of Infection, 2020. **81**(1): p. 107-114.
2. Lyu, W., & Wehby, G. L., et al., *Community use of face masks and COVID-19: Evidence from a natural experiment of state mandates in the US.* Health Affairs, 2020. **39**(8): p. 1419-1425.
3. Samet, J. M., Burke, T. A., Lakdawala, S. S., Lowe, J. J., Marr, C. L., Prather, K. A., et al., *SARS-CoV-2 indoor air transmission is a thread that can be addressed with science.* PNAS, 2021. **118**(45): p. 3-4.
4. *Understanding the Difference*. [cited 2022 10/11]; Available from: https://www.cdc.gov/niosh/npptl/pdfs/understanddifferenceinfographic-508.pdf
5. U.S. Companies Shifted to Make N95 Respirators During COVID. Now, They're Struggling. [cited 2022 10/11]; Available from: https://www.npr.org/2021/06/25/1009858893/u-s-companies-shifted-to-make-n95-respirators-during-covid-now-theyre-struggling
6. Leith, D., L'Orange, C., Volckens, J., et al., *Quantitative Protection Factors for Common Masks and Face Coverings*. Environmental Science & Technology, 2021. **55**(5): p. 1-7.
7. Hao, W., Xu, G., Wang, Y., et al., *Factors influencing the filtration performance of homemade face masks*. JOURNAL OF OCCUPATIONAL AND ENVIRONMENTAL HYGIENE, 2021. **18**(3): p. 2-10.
7 Park, S., Jayaraman, S., et al., *From containment to harm reduction from SARS-CoV-2: a fabric mask for enhanced effectiveness, comfort, and compliance*. The Journal of the Textile Institute. **112**(7): p. 1144-1158.
8 Gerick, A., Militky, J., Venkataraman, M., Steyn, H., Vermaas, J., et al., *The Effect of Mask Style and Fabric Selection on the Comfort Properties of Fabric Masks*
8. Drewnick, F., Pikmann, J., Fachinger, F., Moormann, L., Sprang, F., Borrmann, S., et al., *Aerosol filtration efficiency of household materials for homemade face masks: Influence of material properties, particle size, particle electrical charge, face velocity, and leaks*. Aerosol Science and Technology 2021. **55**(1): p. 2-16.
9. Mueller, A., Fernandez, L., et al., *Assessment of Fabric Masks as Alternatives to Standard Surgical Masks in Terms of Particle Filtration Efficiency*. 2020. p. 1-8.
10. Pei, C., Ou, Q., K., S. C., Chen, S.-C., Pui, D. Y.H., et. al., *Alternative Face Masks Made of Common Materials for General Public: Fractional Filtration Efficiency and Breathability Perspective*. Aerosol and Air Quality Research, 2020. **20**(12): p. 2581-2591.
11. Mirrielees, J. A., Chen, B., Moreno, M. R., Brooks, S. D., et al., *What to Wear: The Filtration Performance of Alternative Materials Used to Construct Do-It-Yourself Masks*. Aerosol and Air Quality Research, 2021. **21**(8). p. 200633.
12. Morais, F. G., Sakano, V. K., de Lima, L. N., Franco, M. A., Reis, D. C., Zanchetta, L. M., et al., *Filtration efficiency of a large set of COVID-19 face masks commonly used in Brazil*. Aerosol Science and Technology, 2021. **55**(9): p. 1028-1041.
13. Patra, S. S., Nath, J., Panda, S., Das, T., Ramasamy, B., et al., *Evaluating the filtration efficiency of commercial facemasks' materials against respiratory aerosol droplets*. JOURNAL OF THE AIR & WASTE MANAGEMENT ASSOCIATION, 2022. **72**(1): p. 3-9.
13 Santarpia, J. L., Herrera, V. L., Rivera, D. N., Ratnesor-Shumate, S., R. St. P., Ackerman, D N., et al., *The size and culturability of patient-generated SARS-CoV-2 aerosol.* Journal of Exposure Science & Environmental Epidemiology, 2022. **32**(3): p. 706-711.

14 Vass, W. B., Lednicky, J. A., Shanker, S. N., Fan, H., Eiguren-Fernandez, A., Wu C.-Y., et al., *Viable SARS-CoV-2 Delta variant detected in aerosols in a residential setting with a self-isolating college student with COVID-19.* Journal of Aerosol Science, 2022. **165**(14): p. 106038-106050.
14. Rogak, S. N., Sipkens, T. A., Guan, M., Nikookar, H., Figueroa, D. V., Wang, J., et al., *Properties of materials considered for improvised masks*. Aerosol Science and Technology, 2021. **55**(4): p. 398-413.
15. Ju, J. T.J., Boisvert, L. N., Zuo, Y. Y., et al., *Face masks against COVID-19: Standards, efficacy, testing and decontamination methods*. Advances in Colloid and Interface Science, 2021. **292**: p. 102435
16. Hinds, W. C. (1999). *Aerosol technology: Properties, behavior, and measurement of airborne particles*. John Wiley & Sons.
17. Kodros, J. K., O'dell, K., Samet, J. M., L'Orange, C., Pierce, J. R., Volckens, J., et al., *Quantifying the Health Benefits of Face Masks and Respirators to Mitigate Exposure to Severe Air Pollution*. GeoHealth, 2021. **5**(9): p. 1-14.
18. Konda, A., Prakash, A., Moss, G. A., Schmoldt, M., Grant, G. D., Guha, S., et al., *Aerosol Filtration Efficiency of Common Fabrics Used in Respiratory Cloth Masks.* ACS NANO, 2020. **14**(5): p. 6339-6347.
19. Good, N., Fedak, K. M., Goble, D., Keisling, A., L'Orange, C., Morton, E., et al., *Respiratory Aerosol Emissions from Vocalization: Age and Sex Differences Are Explained by Volume and Exhaled CO2*. Environmental Science & Technology Letters, 2021. **8**(12): p. 1071-1076.
20. Kwong, L. H., Wilson, R., Kumer, S., Crider, Y. S., Sanchez, Y. R., Rempel, D., Pillarisetti, A., et al., *Review of the Breathability and Filtration Efficiency of Common Household Materials for Face Masks*. ACS NANO, 2021. **15**(4): p. 5904-5924.
21. Konda, A., Prakash, A., Moss, G., Schmoldt, M., Grant, G., Guha, S., et al., *Correction to Aerosol Filtration Efficiency of Common Fabrics Used in Respiratory Cloth Masks*. ACS Nano, 2020. **14**(8): p. 10742-10743
22. Hancock, J. N., Plumley, M. J., Schilling, K., Sheets, D., Wilen, L., et al., *Comment on "Aerosol Filtration Efficiency of Common Fabrics Used in Respiratory Cloth Masks".* ACS Nano, 2020. **14**(9): p. 10758-10763.
23. Rule, A., Ramachandran, G., Koehler, K., et al., *Comment on Aerosol Filtration Efficiency of Common Fabrics Used in Respiratory Cloth Masks: Questioning Their Findings*. ACS Nano, 2020. **14**(9), 10756-10757.
24. Science Brief: Community Use of Masks to Control the Spread of SARS-CoV-2. [cited 2022 10/13]; Available from: https://www.cdc.gov/coronavirus/2019-ncov/science/science-briefs/masking-science-sars-cov2.html

CHAPTER 6 – APPENDICES

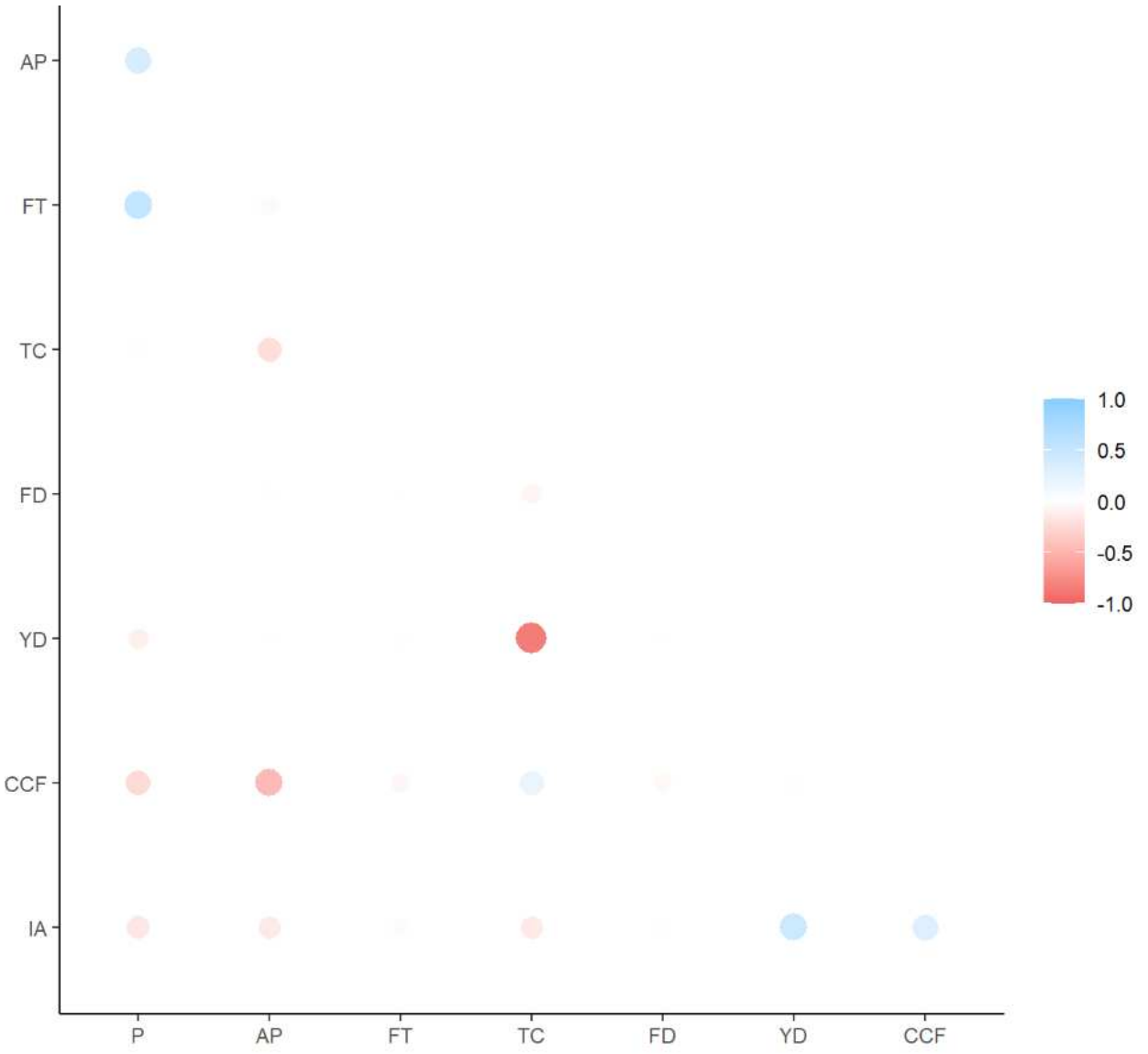

Figure 11: Correlogram containing all eight fabric characteristics. The axis labels are the initials for the following fabric characteristics: "AP" – air permeability, "FT" – fabric thickness, "TC" – thread count, "FD" – fiber diameter, "YD" – yarn diameter, "CCF" – cloth cover factor, "IA" – IR attenuation, "P" – porosity.

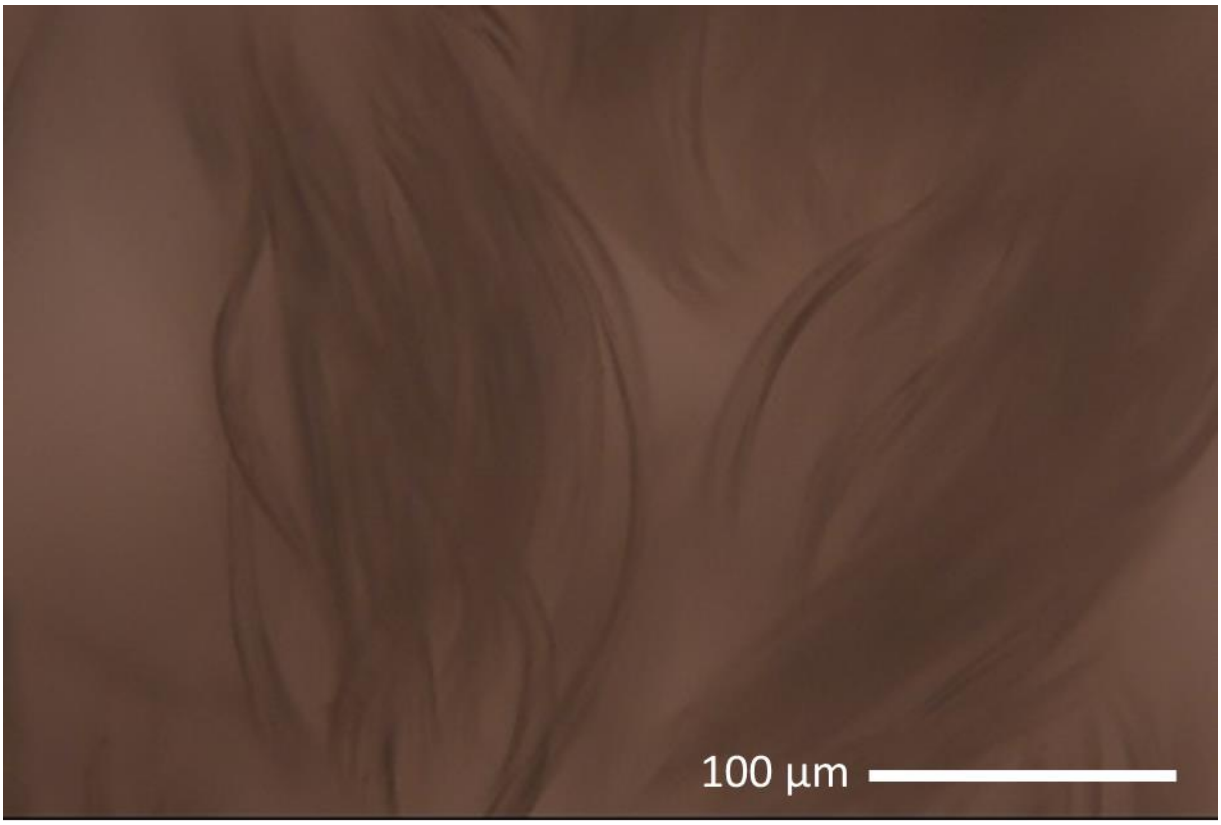

Figure 12: Microscope image of a fabric layer containing synthetic fibers. The fibers are smoother and more uniform in size than natural fibers, allowing for a more precise measurement of particle diameter.

Table 1 : Statistics related to the linear regression run between the following fabric characteristics and FE: thread count, yarn diameter, fiber diameter, cloth cover factor, porosity, air permeability, IR attenuation, and fabric thickness.

Thread Count

diameter	term	estimate	std.error	statistic	p.value	conf.low	conf.high
0.63	intercept	8.24e-02	9.47e-03	8.70	0.0000	6.35e-02	1.01e-01
0.63	slope	1.65e-05	8.20e-06	2.01	0.0488	1.00e-07	3.29e-05
1.99	intercept	2.07e-01	1.92e-02	10.80	0.0000	1.69e-01	2.46e-01
1.99	slope	2.30e-05	1.67e-05	1.38	0.1720	-1.03e-05	5.63e-05
4.12	intercept	4.31e-01	3.25e-02	13.30	0.0000	3.66e-01	4.96e-01
4.12	slope	3.71e-05	2.82e-05	1.32	0.1920	-1.91e-05	9.34e-05
7.97	intercept	7.77e-01	2.36e-02	32.90	0.0000	7.30e-01	8.24e-01
7.97	slope	3.37e-05	2.04e-05	1.65	0.1040	-7.10e-06	7.45e-05

Yarn Diameter

diameter	term	estimate	std.error	statistic	p.value	conf.low	conf.high
0.63	intercept	1.08e-01	0.031900	3.3800	0.001210	0.044200	0.172000
0.63	slope	-6.61e-05	0.000134	-0.4950	0.622000	-0.000333	0.000201
1.99	intercept	2.30e-01	0.064000	3.5900	0.000616	0.102000	0.358000
1.99	slope	-3.69e-05	0.000268	-0.1380	0.891000	-0.000571	0.000497
4.12	intercept	4.00e-01	0.108000	3.7100	0.000420	0.185000	0.615000
4.12	slope	2.35e-04	0.000451	0.5210	0.604000	-0.000665	0.001130
7.97	intercept	7.92e-01	0.079200	10.0000	0.000000	0.634000	0.950000
7.97	slope	3.04e-05	0.000331	0.0918	0.927000	-0.000630	0.000691

Fiber Diameter

diameter	term	estimate	std.error	statistic	p.value	conf.low	conf.high
0.63	intercept	0.18800	0.06310	2.97	5.37e-03	0.0595	0.31600
0.63	slope	-0.00688	0.00422	-1.63	1.12e-01	-0.0155	0.00170
1.99	intercept	0.34000	0.12700	2.69	1.10e-02	0.0833	0.59800
1.99	slope	-0.00881	0.00846	-1.04	3.05e-01	-0.0260	0.00838
4.12	intercept	0.61300	0.23100	2.65	1.20e-02	0.1440	1.08000
4.12	slope	-0.01170	0.01540	-0.76	4.52e-01	-0.0431	0.01960
7.97	intercept	1.02000	0.15200	6.72	1.00e-07	0.7130	1.33000
7.97	slope	-0.01580	0.01020	-1.55	1.29e-01	-0.0365	0.00486

Cloth Cover Factor

diameter	term	estimate	std.error	statistic	p.value	conf.low	conf.high
0.63	intercept	-0.317	0.154	-2.07	4.46e-02	-0.6270	-0.00794
0.63	slope	0.426	0.165	2.58	1.33e-02	0.0933	0.75900
1.99	intercept	-0.908	0.302	-3.00	4.39e-03	-1.5200	-0.29900
1.99	slope	1.190	0.325	3.66	6.77e-04	0.5340	1.84000
4.12	intercept	-1.680	0.458	-3.67	6.56e-04	-2.6000	-0.75700
4.12	slope	2.260	0.493	4.58	3.82e-05	1.2600	3.25000
7.97	intercept	-1.040	0.370	-2.82	7.21e-03	-1.7900	-0.29700
7.97	slope	1.940	0.398	4.89	1.39e-05	1.1400	2.74000

Porosity

diameter	term	estimate	std.error	statistic	p.value	conf.low	conf.high
0.63	intercept	0.209	0.0826	2.53	1.38e-02	0.044	0.3740
0.63	slope	-0.159	0.1130	-1.41	1.64e-01	-0.384	0.0665
1.99	intercept	0.501	0.1630	3.08	3.00e-03	0.177	0.8260
1.99	slope	-0.382	0.2220	-1.72	9.02e-02	-0.825	0.0615
4.12	intercept	0.973	0.2680	3.63	5.53e-04	0.438	1.5100
4.12	slope	-0.708	0.3660	-1.93	5.73e-02	-1.440	0.0227
7.97	intercept	1.050	0.2030	5.18	2.20e-06	0.647	1.4600
7.97	slope	-0.344	0.2770	-1.24	2.19e-01	-0.898	0.2100

Air Permeability

diameter	term	estimate	std.error	statistic	p.value	conf.low	conf.high
0.63	intercept	0.13900	0.014800	9.38	0.00e+00	0.10900	0.16800
0.63	slope	-0.00258	0.000701	-3.68	4.99e-04	-0.00398	-0.00118
1.99	intercept	0.33500	0.027600	12.10	0.00e+00	0.27900	0.39000
1.99	slope	-0.00622	0.001310	-4.75	1.29e-05	-0.00884	-0.00360
4.12	intercept	0.65000	0.043800	14.80	0.00e+00	0.56200	0.73700
4.12	slope	-0.01080	0.002080	-5.18	2.70e-06	-0.01490	-0.00661
7.97	intercept	0.90500	0.035300	25.60	0.00e+00	0.83400	0.97500
7.97	slope	-0.00570	0.001680	-3.40	1.20e-03	-0.00905	-0.00235

IR Attenuation

diameter	term	estimate	std.error	statistic	p.value	conf.low	conf.high
0.63	intercept	-0.02310	0.031200	-0.739	4.63e-01	-0.08580	0.03960
0.63	slope	0.00276	0.000667	4.130	1.39e-04	0.00142	0.00410
1.99	intercept	-0.02450	0.059300	-0.412	6.82e-01	-0.14400	0.09470
1.99	slope	0.00592	0.001270	4.670	2.40e-05	0.00337	0.00847
4.12	intercept	-0.01010	0.088200	-0.114	9.10e-01	-0.18700	0.16700
4.12	slope	0.01130	0.001890	5.970	3.00e-07	0.00748	0.01510
7.97	intercept	0.54100	0.069100	7.820	0.00e+00	0.40200	0.68000
7.97	slope	0.00642	0.001480	4.340	7.07e-05	0.00345	0.00939

Fabric Thickness

diameter	term	estimate	std.error	statistic	p.value	conf.low	conf.high
0.63	intercept	0.032700	2.06e-02	1.58	1.18e-01	-8.56e-03	0.073900
0.63	slope	0.000124	3.85e-05	3.22	1.99e-03	4.72e-05	0.000201
1.99	intercept	0.126000	4.17e-02	3.01	3.71e-03	4.23e-02	0.209000
1.99	slope	0.000202	7.79e-05	2.59	1.17e-02	4.64e-05	0.000358
4.12	intercept	0.301000	6.88e-02	4.37	4.56e-05	1.63e-01	0.438000
4.12	slope	0.000326	1.29e-04	2.54	1.36e-02	6.93e-05	0.000583
7.97	intercept	0.680000	4.98e-02	13.70	0.00e+00	5.81e-01	0.780000
7.97	slope	0.000258	9.29e-05	2.77	7.20e-03	7.23e-05	0.000444

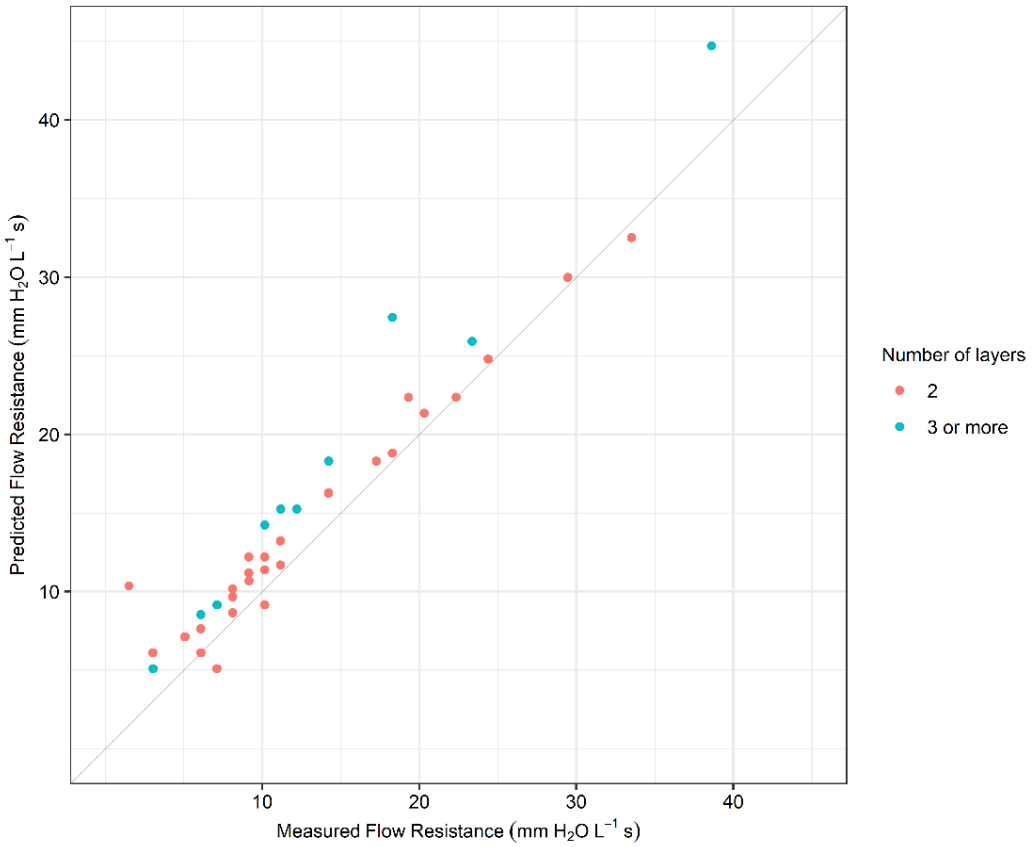

Figure 13: Comparing the flow resistance measured from each mask (x-axis) to that predicted for each mask using the flow resistance of its component layers (y-axis). The diagonal line, y=x, represents perfect agreement between the measured and predicted flow resistance.

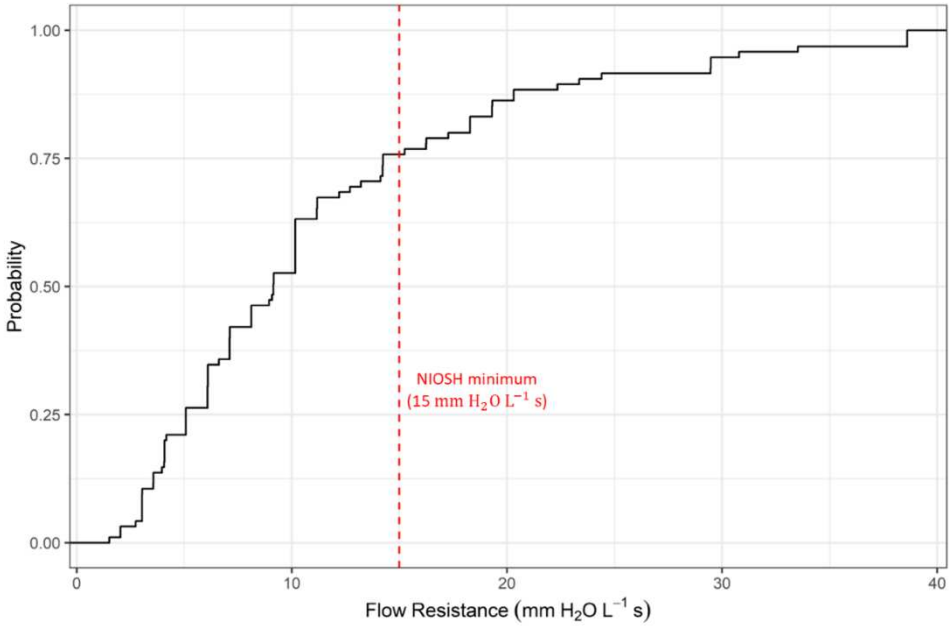

Figure 14: Empirical cumulative distribution of flow resistance in the set of 50 masks. 38 of the 50 masks meet the NIOSH minimum criteria of 15 mm H_2O L^{-1} s.

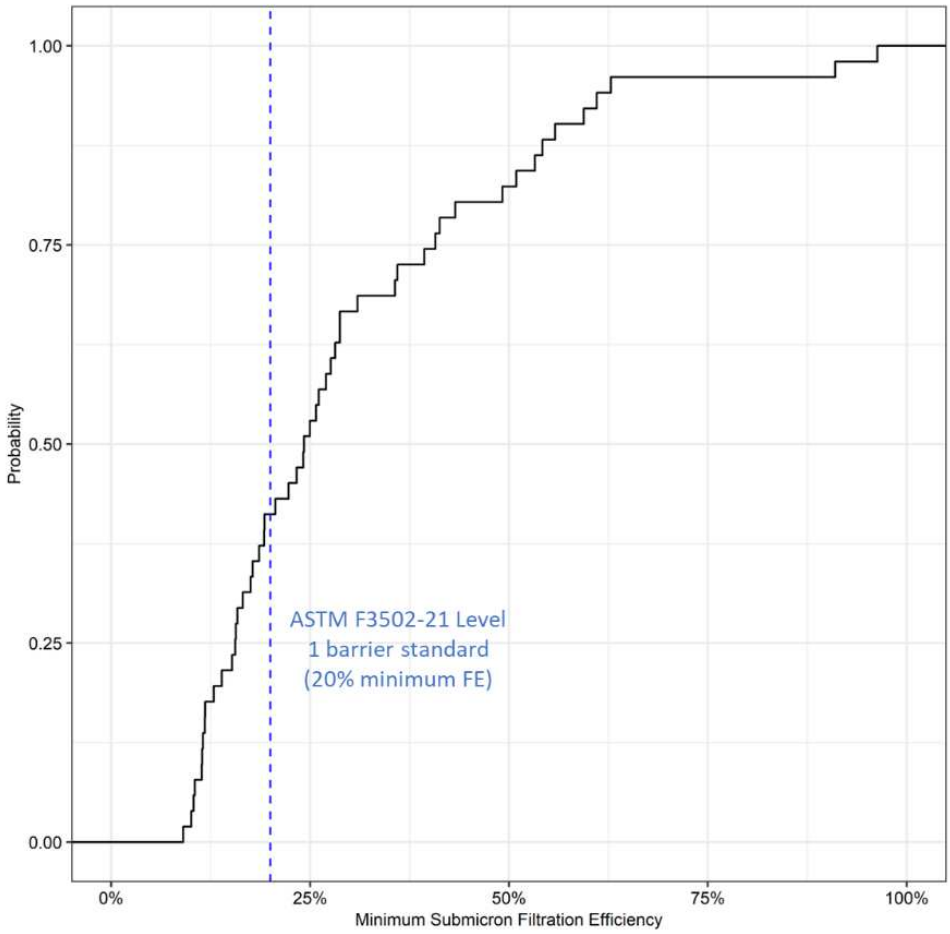

Figure 15: Empirical cumulative distribution of the minimum FE for particle diameters less than one micron in the set of 50 masks. 29 of the 50 masks meet the ASTM F3502-21 Level 1 barrier standard of a minimum FE of 20% in the submicron range.

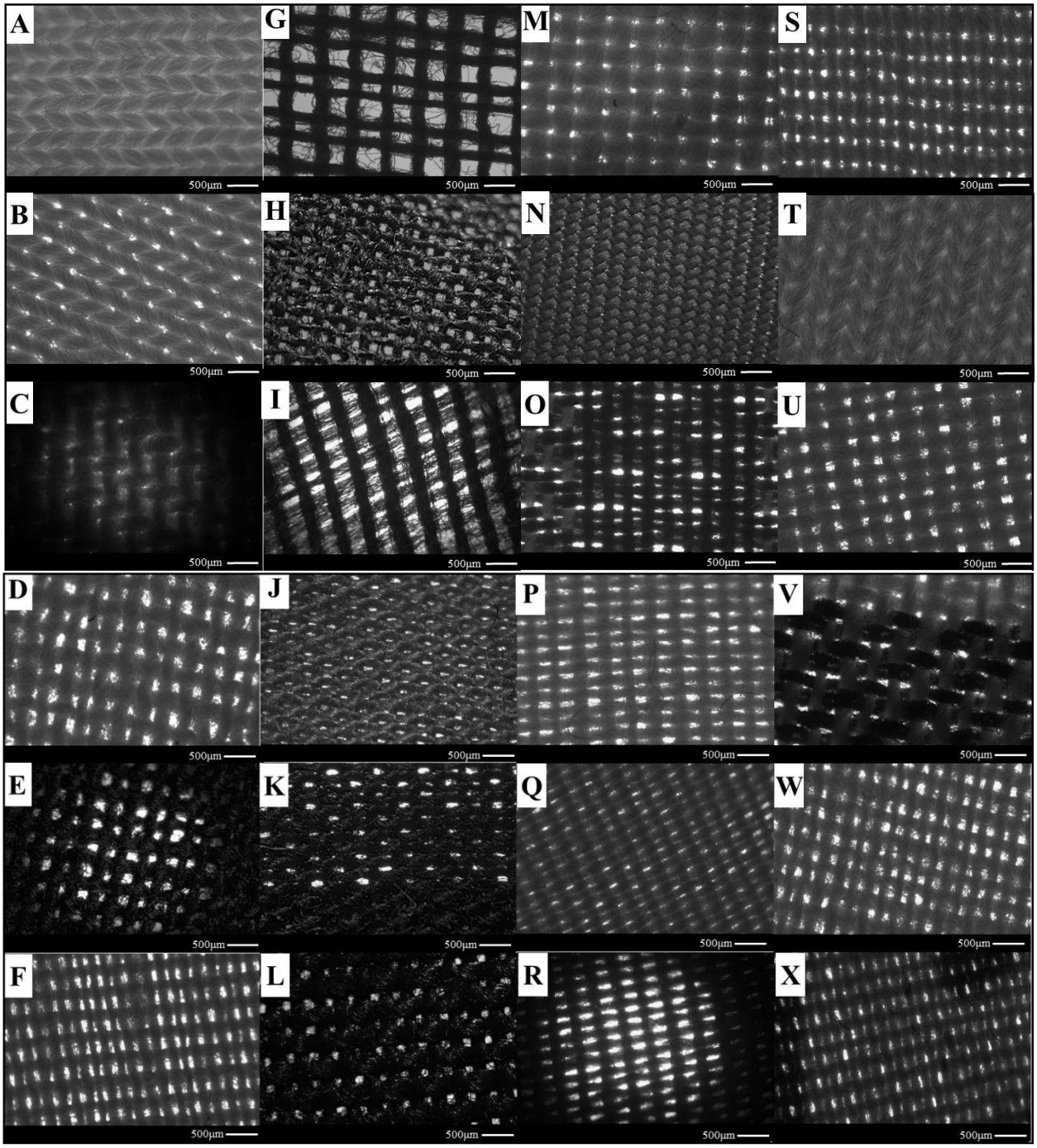
A
G
M
S
B
H
N
T
C
I
O
U
D
J
P
V
E
K
Q
W
F
L
R
X
500µm

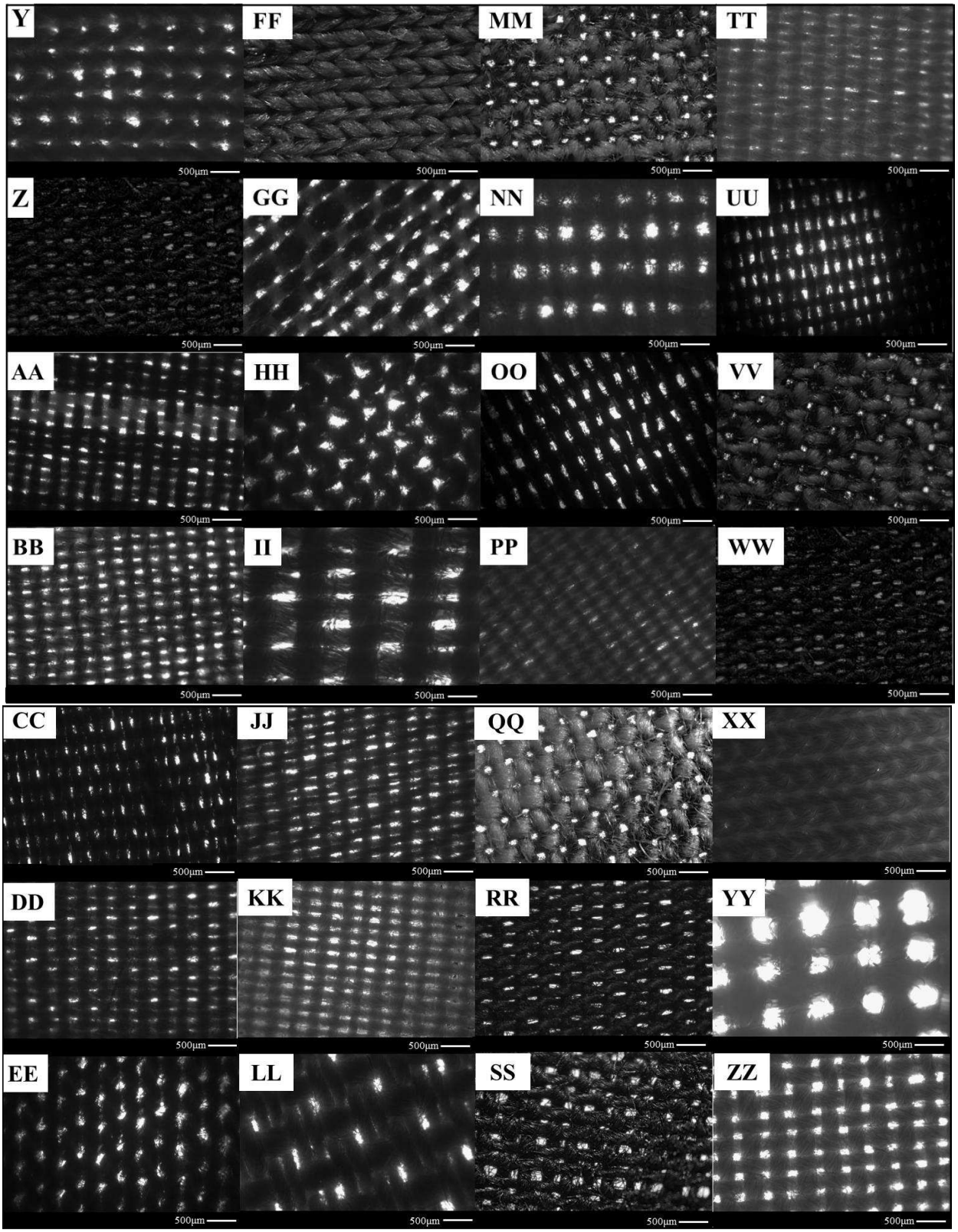

Figure 16: Microscope images of the individual fabric layers.

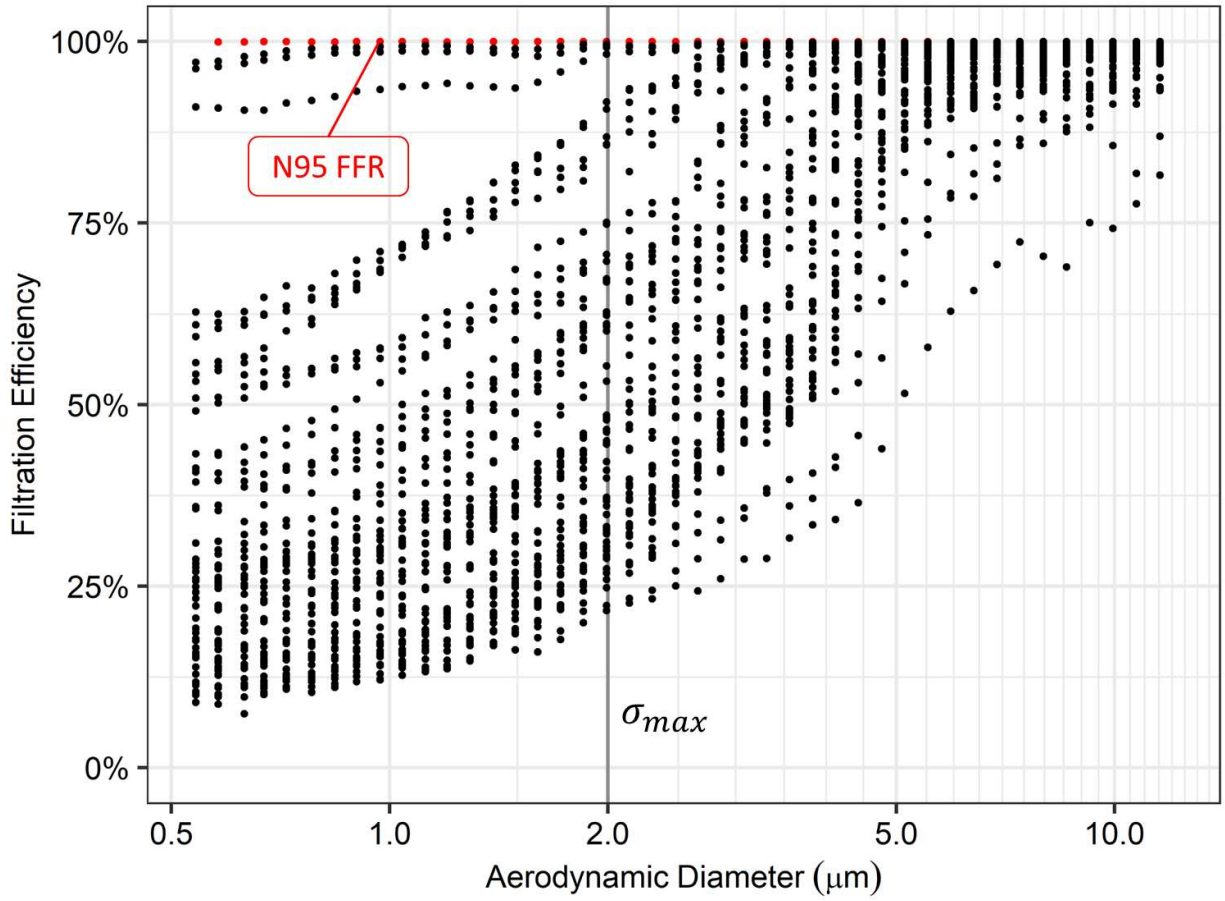

Figure 17: Showing Figure 4 without the three-parameter nonlinear regression that creates smooth curves for each mask out of the FE data.

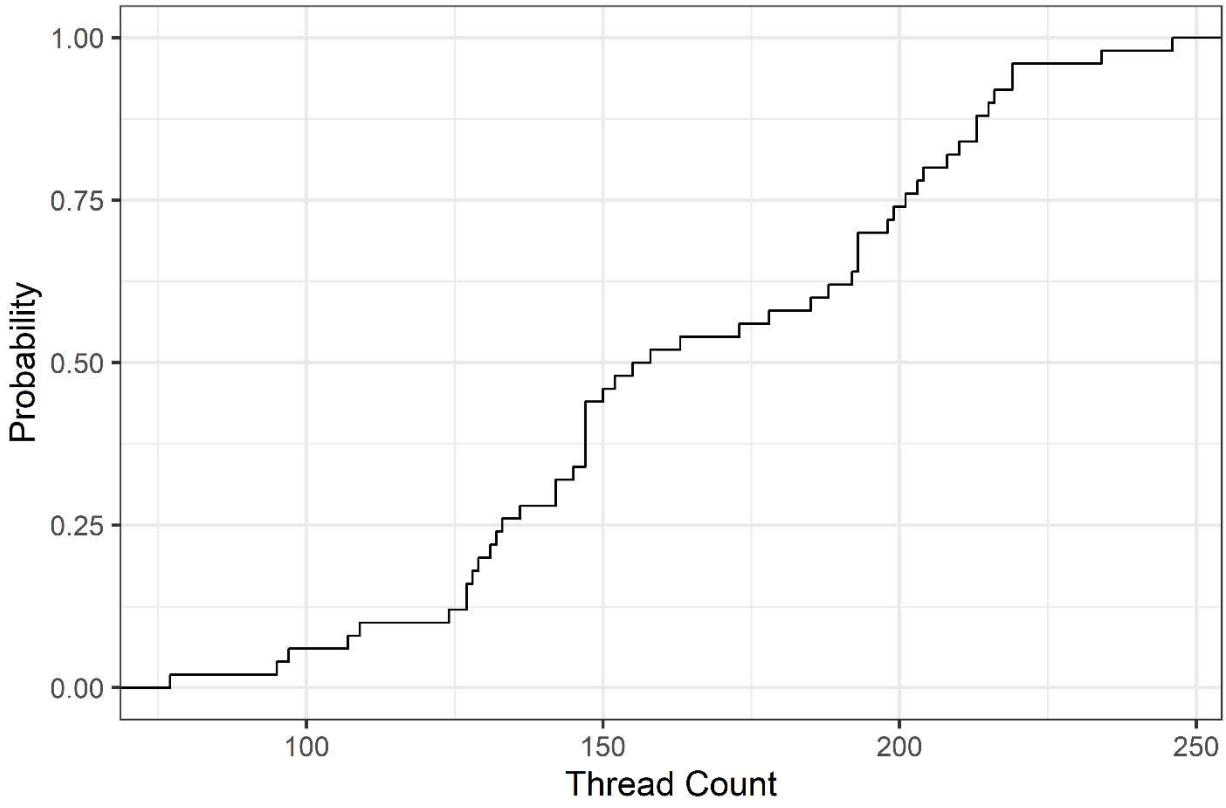
1.00
0.75
0.50
0.25
0.00
Probability
100
150
200
250
Thread Count

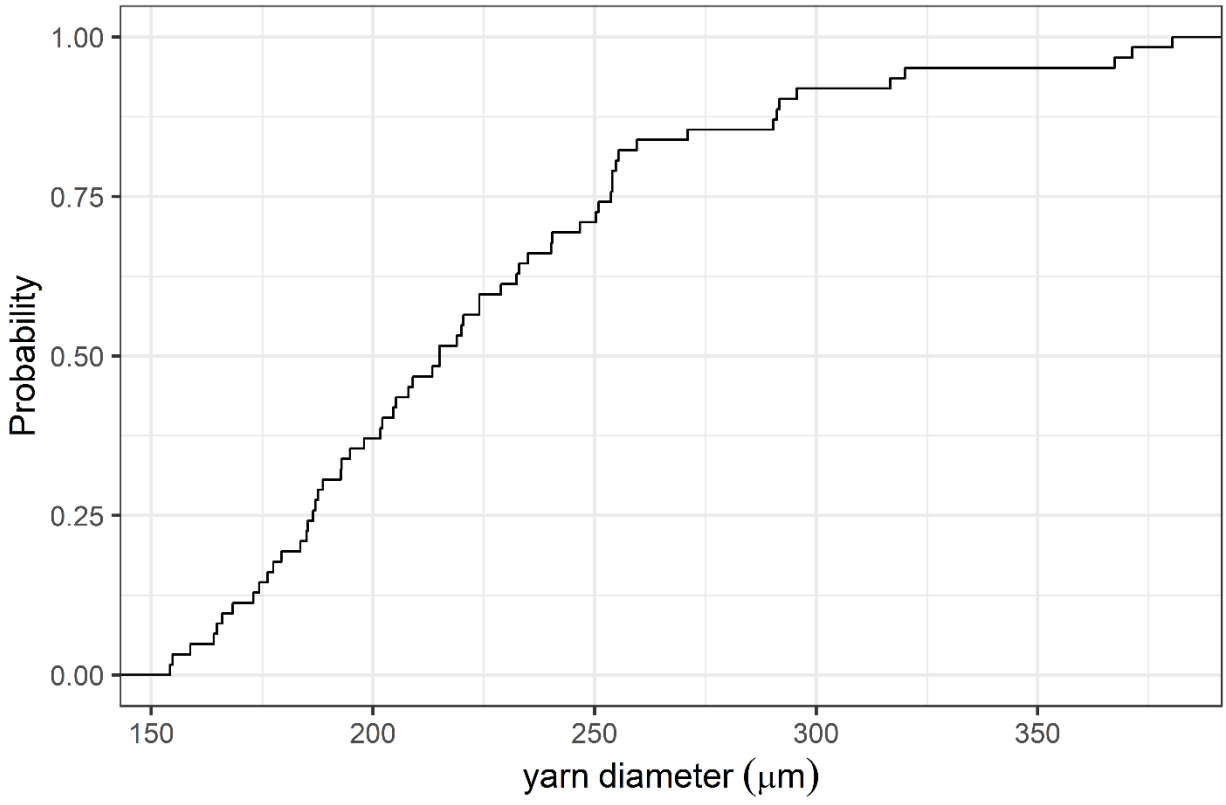
1.00
0.75
0.50
0.25
0.00
Probability
150
200
250
300
350
yarn diameter (μm)

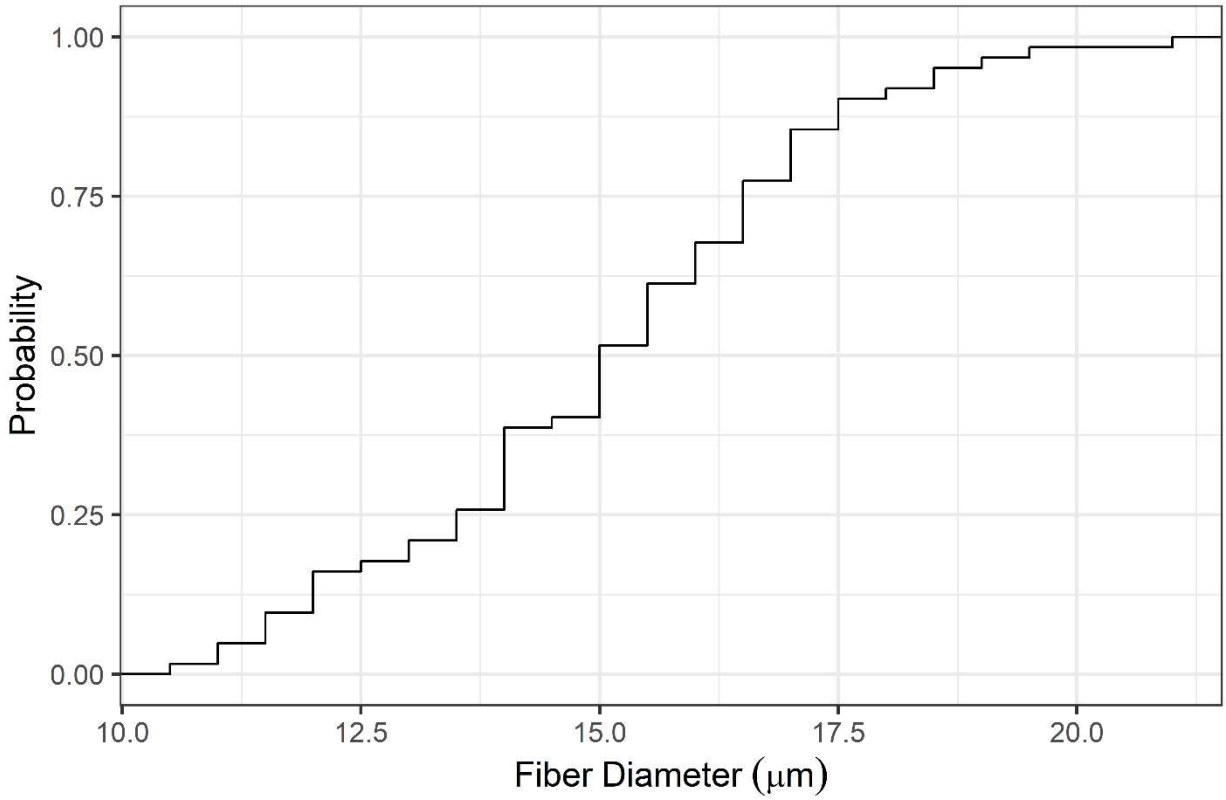
1.00
0.75
0.50
0.25
0.00
Probability
10.0
12.5
15.0
17.5
20.0
Fiber Diameter (μm)

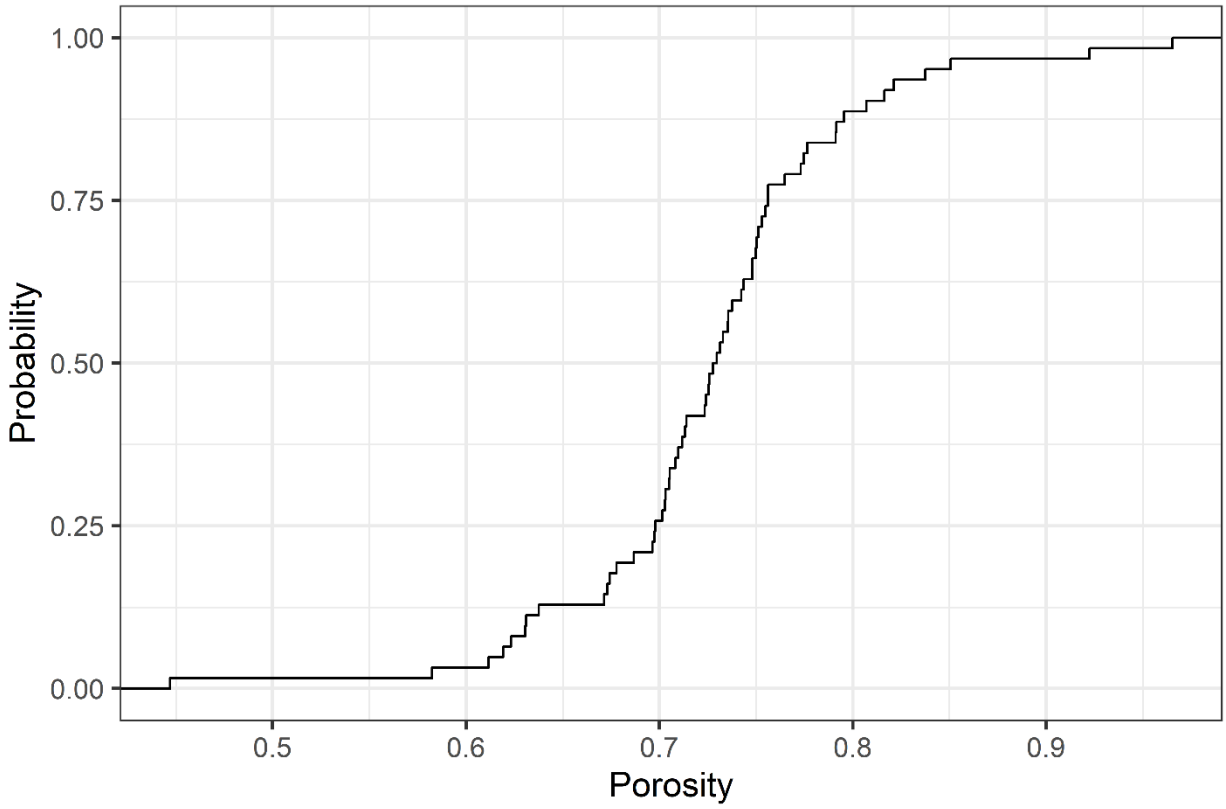
1.00
0.75
0.50
0.25
0.00
Probability
0.5
0.6
0.7
0.8
0.9
Porosity

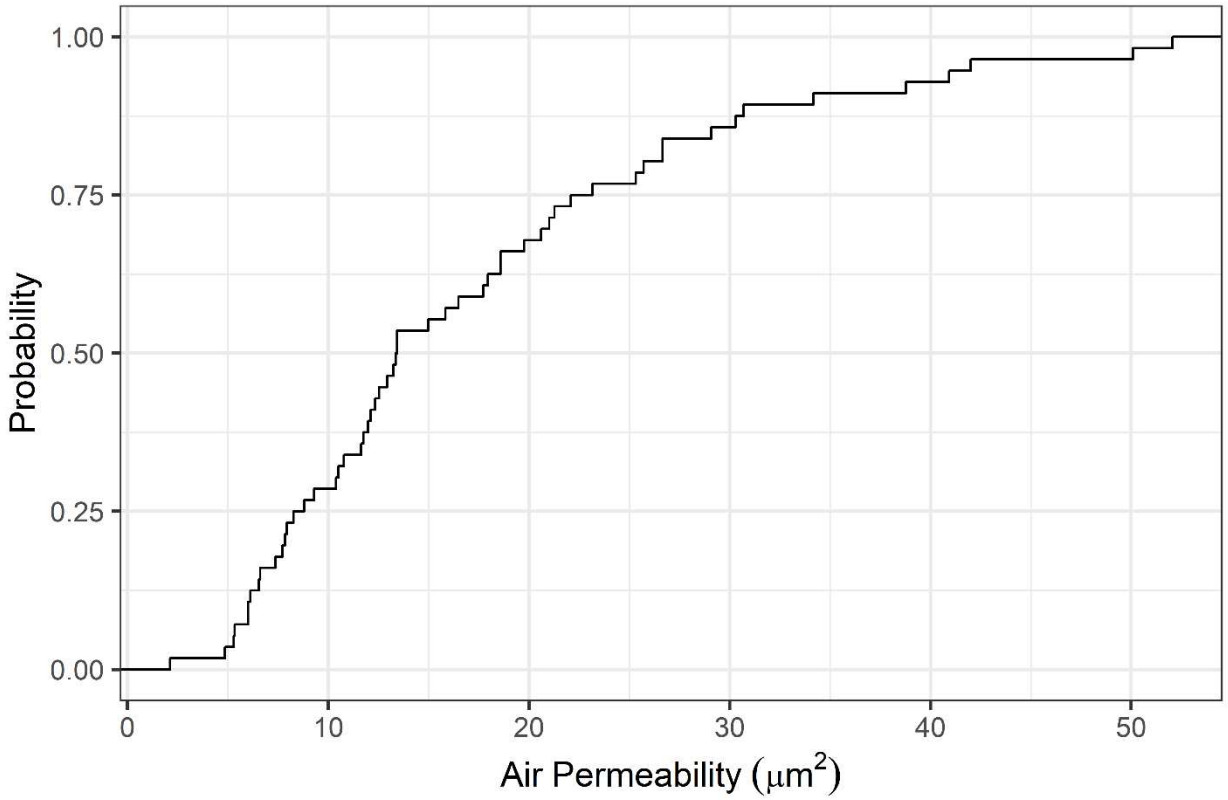
1.00
0.75
0.50
0.25
0.00
Probability
0
10
20
30
40
50
Air Permeability (μm²)

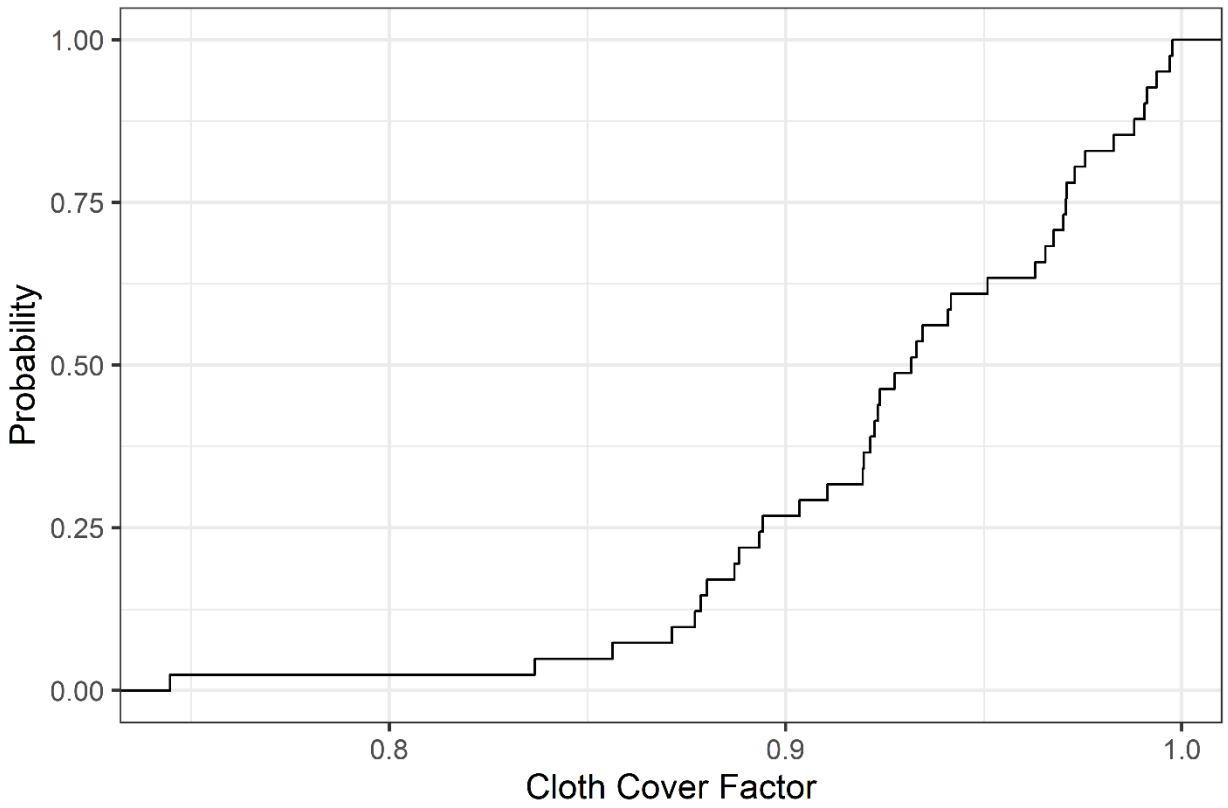
1.00
0.75
0.50
0.25
0.00
Probability
0.8
0.9
1.0
Cloth Cover Factor

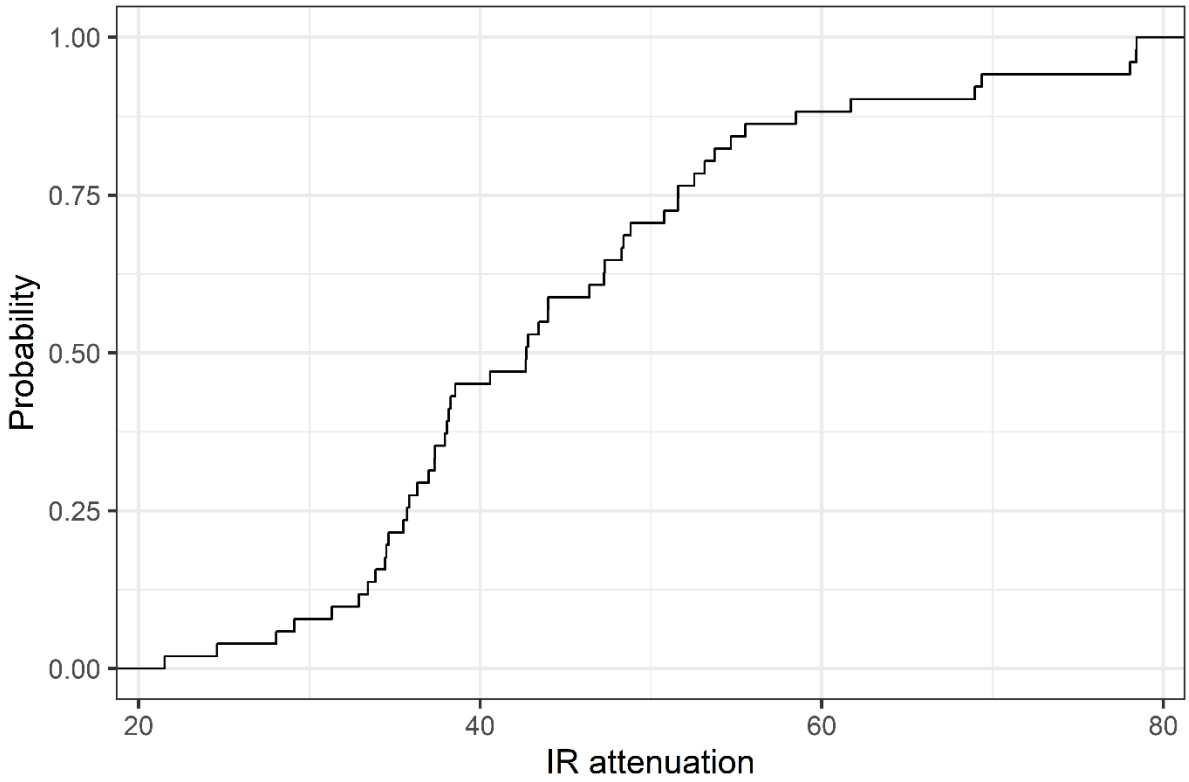

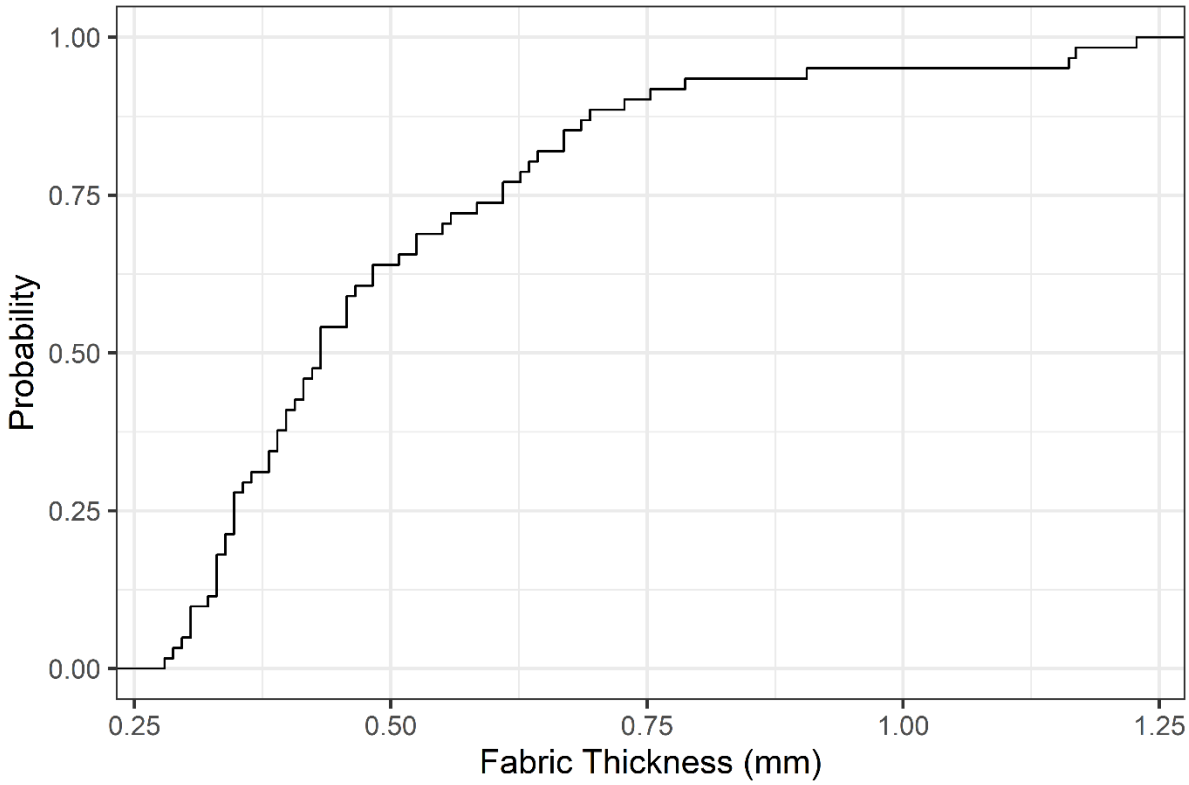

Figure 18: Empirical distribution function plots of all eight characteristics studied